Molecular Pharmacology Fast Forward. Published on September 29, 2017 as DOI: 10.1124/mol.117.110379
This article has not been copyedited and formatted. The final version may differ from this version.

RVX-297, a BET bromodomain inhibitor, has therapeutic effects in preclinical models of acute inflammation and autoimmune disease

Ravi Jahagirdar, Sarah Attwell, Suzana Marusic, Alison Bendele, Narmada Shenoy, Kevin G. McLure, Dean Gilham, Karen Norek, Henrik C. Hansen, Raymond Yu, Jennifer Tobin, Gregory S. Wagner, Peter R. Young, Norman C.W. Wong, Ewelina Kulikowski

Resverlogix Corp., Suite 300, 4820 Richard Road SW, Calgary, Alberta T3E 6L1, Canada (RJ, SA, KGM, DG, KN, HCH, RY, JT, GSW, PRY, NCWW, EK).

Hooke Laboratories Inc., 439 South Union Street, Lawrence, MA 01843, USA (SM).

Bolder BioPATH Inc., 5541 Central Avenue, Boulder, CO 80301, USA (AB).

Aravasc Inc., 1230 Bordeaux Drive, Sunnyvale, CA 94089, USA (NS).

Molecular Pharmacology Fast Forward. Published on September 29, 2017 as DOI: 10.1124/mol.117.110379
This article has not been copyedited and formatted. The final version may differ from this version.

Running Title: RVX-297 ameliorates inflammation and autoimmune disease

Corresponding Author: Dr. Ravi Jahagirdar, Resverlogix Corp., Suite 300, 4820 Richard Road SW, Calgary, Alberta T3E 6L1, Canada, Phone: 587-390-7889, Fax: 403-256-8495, E-mail: ravi@resverlogix.com

Number of text pages: 28

Number of tables: 6

Number of figures: 8

Number of references: 61

Number of words in Abstract: 247

Number of words in Introduction: 737

Number of words in Discussion: 1,199

Non-standard Abbreviations:

BMDM: bone marrow-derived macrophage; BET: bromodomain and extra-terminal domain containing protein; BD: bromodomain; BETi: BET bromodomain inhibitor; BRD: bromodomain containing; CAIA: collagen antibody induced arthritis; CAS: clinical arthritis score; CFA: complete Freund's adjuvant; ChIP: chromatin immunoprecipitation; CIA: collagen-induced arthritis; CNS: central nervous system; C_T: threshold cycle; CVD: cardiovascular disease; DMEM: Dulbecco's modified Eagle's medium; EAE: experimental autoimmune encephalomyelitis; ELISA: enzyme-linked immunosorbent assay; GM-CSF: granulocyte-macrophage colony-stimulating factor; IACUC:

Molecular Pharmacology Fast Forward. Published on September 29, 2017 as DOI: 10.1124/mol.117.110379
This article has not been copyedited and formatted. The final version may differ from this version.

Institutional Animal Care and Use Committee; IL: interleukin; IFA: incomplete Freund's adjuvant; IFNγ: interferon gamma; LPS: lipopolysaccharide; MAP: multi-analyte profiling; MCP: monocyte chemotactic protein; MMP: matrix metalloproteinase; MMS: mean maximum score; MOG: myelin oligodendrocyte glycoprotein; MS: multiple sclerosis; NF-κB: nuclear factor kappa-light-chain-enhancer of activated B cells; NF-κBia: NF-κB inhibitor alpha; PBMC: peripheral blood mononuclear cell; PD: pharmacodynamic; PK: pharmacokinetic; PMA: phorbol 12-myristate 13-acetate; P-TEFb: positive transcription elongation factor b; RA: rheumatoid arthritis; RANKL: receptor activator of nuclear factor kappa-B ligand; RANTES: regulated on activation, normal T-cell expressed and secreted; T_H: T helper cells; TNFα: tumor necrosis factor alpha; VCAM-1: vascular cell adhesion molecule

Molecular Pharmacology Fast Forward. Published on September 29, 2017 as DOI: 10.1124/mol.117.110379
This article has not been copyedited and formatted. The final version may differ from this version.

ABSTRACT

Bromodomain and extra-terminal (BET) domain proteins are chromatin adapters that bind acetylated histone marks via two tandem bromodomains (BD1 and BD2) to regulate gene transcription. BET proteins are involved in transcriptional reprogramming in response to inflammatory stimuli. BET bromodomain inhibitors (BETi) that are non-selective for BD1 or BD2 have recognized anti-inflammatory properties *in vitro* and counter pathology in models of inflammation or autoimmune disease. While both BD1 and BD2 bind acetylated histone residues, they may independently regulate expression of BET sensitive genes. Here we characterized the ability of RVX-297, a novel orally active BETi with selectivity for BD2, to modulate inflammatory processes *in vitro, in vivo,* and *ex vivo*. RVX-297 suppressed inflammatory gene expression in multiple immune cell types in culture. Mechanistically, RVX-297 displaced BET proteins from the promoters of sensitive genes and disrupted recruitment of active RNA polymerase II, a property shared with pan-BETi that non-selectively bind BET bromodomains. In the lipopolysaccharide (LPS) model of inflammation, RVX-297 reduced pro-inflammatory mediators assessed in splenic gene expression and serum proteins. RVX-297 also countered pathology in three rodent models of polyarthritis: rat and mouse collagen induced arthritis (rCIA and mCIA) and mouse collagen antibody induced arthritis (mCAIA). Further, RVX-297 prevented murine experimental autoimmune encephalomyelitis (EAE; a model of human multiple sclerosis) disease development when administered prophylactically, and reduced hallmarks of pathology when administered therapeutically. We show for the first time that a BD2 selective BETi

Molecular Pharmacology Fast Forward. Published on September 29, 2017 as DOI: 10.1124/mol.117.110379
This article has not been copyedited and formatted. The final version may differ from this version.

maintains anti-inflammatory properties and is effective in preclinical models of acute inflammation and autoimmunity.

Molecular Pharmacology Fast Forward. Published on September 29, 2017 as DOI: 10.1124/mol.117.110379
This article has not been copyedited and formatted. The final version may differ from this version.

1 INTRODUCTION

Proinflammatory stimuli induce rapid transcriptional responses that are essential for host defense from infection. Regulation of inflammatory gene expression is coordinated and tightly controlled to both elicit and retract the response. Although inflammation is critical for immune defense, the process is pathological if exaggerated, chronically sustained or directed against the individual's own tissue to generate an autoimmune condition. An inflammatory response involves a variety of cell types and expression of inflammatory mediators such as cytokines and chemokines. Cytokines, including interleukin-6 (IL-6) and interleukin-1β (IL-1β), have potent proinflammatory actions that contribute to the pathogenesis of autoimmune disorders (Choy and Panayi, 2001). IL-6 also stimulates differentiation of naïve T-cells into T_H17 cells that promote amplification of the inflammatory response in a feed forward mechanism (Dienz and Rincon, 2009). Interleukin 17 (IL-17) producing T helper cells (T_H17 cells) play a critical role in development of autoimmune disorders including rheumatoid arthritis (RA) and multiple sclerosis (MS). In autoimmune disorders, IL-17 mediates tissue inflammation through signal transduction that recruits and activates neutrophils and macrophages, and promotes expression of proinflammatory chemokines and cytokines (Kolls and Linden, 2004; Ye et al., 2001). Current evidence suggest IL-17 plays an active role in inflammatory diseases, autoimmune disorders, and cancer (Kolls and Linden, 2004).

Extensive transcriptional reprogramming is invoked by proinflammatory stimuli (Brown et al., 2014). Epigenetic modifications to chromatin provide a framework for the rapid

Molecular Pharmacology Fast Forward. Published on September 29, 2017 as DOI: 10.1124/mol.117.110379
This article has not been copyedited and formatted. The final version may differ from this version.

alterations in gene expression required for immune cell activation and differentiation (Wei et al., 2009). Epigenetics regulate gene expression through covalent modifications of chromatin that impact chromatin structure and the recruitment of transcriptional complexes. Histone acetylation is one such modification associated with active gene transcription. Acetylation occurs on lysine residues, which are recognized by chromatin readers such as the bromodomain and extra-terminal (BET) family of proteins (BRD2, BRD3, BRD4, and the testis specific BRDT). BET proteins contain two tandem bromodomains, BD1 and BD2, that interact with acetylated lysines on histone tails and recruit transcriptional machinery to regulate gene expression (Filippakopoulos et al., 2012). Pharmacological inhibitors of BET BDs that bind BD1 and BD2 with similar affinity (pan-BETi) can suppress inflammatory gene expression; they prevent BET protein associations with acetylated histones at the promoters of genes encoding inflammatory cytokines (Bandukwala et al., 2012; Brown et al., 2014; Nicodeme et al., 2010). Both genetic approaches and pan-BETi studies have demonstrated that BET proteins are critical for inflammatory responses in macrophages, including the expression of IL-6 and other key inducible cytokines and chemokines (Nicodeme et al., 2010). Roles for BET proteins in both acute inflammatory responses (Belkina et al., 2013; Nicodeme et al., 2010) as well as autoimmune pathology involving T_H17 cell differentiation (Mele et al., 2013) have been established. BET proteins are not only involved in differentiation of naïve CD4+ T-cells to T_H17 cells, but also in activation of previously differentiated T_H17 cells (Mele et al., 2013). Further, T-cell mediated immunity involves maturation of dendritic cells, which have also been linked to autoimmune disease (Baumgart and Carding, 2007). Dendritic cells play a stabilizing

Molecular Pharmacology Fast Forward. Published on September 29, 2017 as DOI: 10.1124/mol.117.110379
This article has not been copyedited and formatted. The final version may differ from this version.

role in the immune response and induce T-cell immunity upon maturation, whereas immature cells promote immune tolerance. A pan-BETi can impair full maturation of monocyte derived dendritic cells, resulting in decreased induction of proinflammatory T-cells (Toniolo et al., 2015). Hence several lines of evidence indicate BETi have strong therapeutic potential to suppress inflammatory processes that underlie autoimmune disorders.

Studies have shown that BD selective BETi modify different transcriptional outcomes compared to non-selective BETi (Gacias et al., 2014; Picaud et al., 2013), implying that BD selectivity may have differential biological consequences that impact inflammation. RVX-297 is a novel, orally bioavailable BETi that has 47-58 fold greater affinity for BD2 than for BD1 in the BET family of proteins (Kharenko et al., 2016). In this report we characterize the anti-inflammatory properties of RVX-297, and demonstrate for the first time that a BD2 selective BETi impacts gene expression and cellular function in immune cell types that are involved in inflammation and autoimmunity including macrophages, T-cells, B-cells, and synovial fibroblasts. We also investigate efficacy of RVX-297 in preclinical models of endotoxemia, polyarthritis (Bendele, 2001), and T-cell-mediated autoimmune disease with features of MS (Thakker et al., 2007). Our results demonstrate that BD2 selective inhibition of BET proteins has anti-inflammatory properties *in vitro* and in animal models of autoimmune disease. Based on this data, we suggest that selective inhibition of BD2 has potential in ameliorating autoimmune disorders by simultaneously modulating inflammatory factors in multiple cell types.

Molecular Pharmacology Fast Forward. Published on September 29, 2017 as DOI: 10.1124/mol.117.110379
This article has not been copyedited and formatted. The final version may differ from this version.

2 MATERIALS AND METHODS:

2.1 Materials

I-BET762, JQ1, and RVX-297 were synthesized as previously described (Filippakopoulos et al., 2010; Hansen, 2011; Nicodeme et al., 2010). Dexamethasone and FTY720 were obtained from commercial sources.

2.2 U937 cell treatment

U937 cells (ATCC, Manassas, VA) were differentiated to macrophage-like cells with 60 ng/mL phorbol 12-myristate 13-acetate (PMA) for 3 days. Cells were pretreated for 1 hour with RVX-297 or DMSO without PMA prior to the addition of LPS (1 µg/mL). Cells were incubated for 3 hours before gene expression analysis by real-time PCR. Each data point was derived from 3 biological replicates, and results determined in 3 independent experiments.

2.3 Primary B-cell isolation and treatment

Spleens from C57/Bl6 mice were rinsed in cold PBS and disrupted under a syringe plunger. The cell suspension was passed through a 20 gauge syringe 3 times and filtered through a 50 µm filcom. Cells were pelleted by centrifugation, then resuspended in RBC lysis solution. Cells were pelleted again, and resuspended in isolation buffer (Ca/Mg free PBS with 2 mM EDTA and 2% FBS). B-cells were isolated using mouse CD43 beads (Life Technologies) according to the manufacturer's instructions. Cells

Molecular Pharmacology Fast Forward. Published on September 29, 2017 as DOI: 10.1124/mol.117.110379
This article has not been copyedited and formatted. The final version may differ from this version.

were plated at 15,000 cells/well in 96-well format in RPMI containing 10% FBS, and treated with RVX-297 or DMSO, LPS (1 µg/mL) and ionomycin (1 µM). Incubation was maintained for 3 hours, followed by gene expression analysis. Results were verified in an independent experiment.

2.4 IL-17 expression

IL-17 gene expression was analyzed in human peripheral blood mononuclear cells (PBMCs). Briefly, PBMCs (Cellular Technologies Ltd, Shaker Heights, OH) were thawed in OpTmizer T cell expansion media (Life Technologies) supplemented with 20 ng/mL of IL-2 (Sigma, St. Louis, MO). Cells were pelleted by centrifugation and resuspended in media recommended by the supplier. Cells were pre-treated with RVX-297 or DMSO for 1 hour, then media containing OKT3 (Ebiosciences, San Diego, CA) was added at a final concentration of 1 µg/mL. Incubation was continued for 3 hours. IL-17 gene expression was analyzed by real-time PCR. Each data point was derived from 3 biological replicates and results determined in 6 independent experiments.

2.5 MCP1 assay

Cryopreserved PBMCs (Cellular Technologies Ltd, Shaker Heights, OH) were plated in 96-well format in RPMI media (Life Technologies) containing 10% FBS. Cells were treated for 3 hours with each condition in triplicate before harvesting for gene expression analysis by real-time PCR. RVX-297 mediated repression of MCP1 was verified in 4 independent experiments as well as in PBMCs from 3 different donors.

Molecular Pharmacology Fast Forward. Published on September 29, 2017 as DOI: 10.1124/mol.117.110379
This article has not been copyedited and formatted. The final version may differ from this version.

2.6 Mouse bone marrow-derived macrophage isolation and treatment

Primary bone marrow derived macrophages (BMDMs) were isolated from mouse femurs. Briefly, femurs from 6 week old C57/Bl6 mice were cut with a scalpel at both ends and flushed with RPMI media. Cells were washed and resuspended in media supplemented with 20% FBS, 40 ng/mL GM-CSF and 5 ng/mL IL-3, then allowed to differentiate for 6 days. Cells were re-plated in 24-well format (200,000 cells/well) for further treatments. Each treatment condition was performed in triplicate. Expression of IL-6 and IL-1β were analyzed by real-time PCR. Results were verified in an independent experiment.

2.7 Human rheumatoid arthritis synovial fibroblasts

Synovial fibroblasts isolated from the knee of arthritic patients (Asterand Bioscience, Detroit, MI) were plated at 6,000 cells/well in 96-well format in DMEM containing 10% FBS. Fibroblasts were treated identically to U937 cells, except stimulation was induced with 30 ng/mL TNFα. Real time PCR was performed after 24 hours of treatment. Representative data involving 3 biological replicates per treatment group are shown. The experiment was performed 4 times, and results were verified in cells derived from a different donor.

2.8 Real-time PCR

mRNA was isolated from cell culture systems using Catcher Plus kits (Life Technologies) or from tissue samples using Trizol (Life Technologies) according to the manufacturer's instructions. Gene expression was measured by TaqMan™ based real-

Molecular Pharmacology Fast Forward. Published on September 29, 2017 as DOI: 10.1124/mol.117.110379
This article has not been copyedited and formatted. The final version may differ from this version.

time PCR using the RNA UltraSense One-Step qRT-PCR System as described previously (Gilham et al., 2016; McLure et al., 2013). mRNA levels were measured relative to an endogenous control on 7500 or ViiA-7 Real Time PCR Instruments (Applied Biosystems).

2.9 Chromatin immunoprecipitation (ChIP)

BMDMs were plated in 10 cm dishes $6x10^6$ cells/plate. After 1 day, cells were treated with compound for 1 hour; LPS (1 μg/mL final concentration) and RVX-297 (10 μM) or DMSO (0.1%) were added and incubations were continued for 3 hours. ChIP was performed essentially as previously published (McCarthy et al., 2003; Nicodeme et al., 2010). Briefly, cells were crosslinked with 1% formaldehyde for 10 minutes before quenching with glycine. Chromatin was sheared by sonication and insoluble debris removed by centrifugation. Immunoprecipitation was performed with 500 μg protein and 2 μg of BRD antibodies (Bethyl Labs BRD2 a302-583a, BRD3 a302-368a, BRD4 a301-985a), RNA polymerase II (Abcam ab5095), tetra-acetylated Histone H4 (Millipore 06-866), or IgG (Sigma I5006). A corresponding input sample was treated equally. After de-crosslinking, DNA was isolated by phenol chloroform extraction, and real-time PCR was performed using Power SYBR Green reagent for detection (Applied Biosystems). PCR primer sequences were published by Nicodeme *et al.* (Nicodeme et al., 2010), and the fold difference was calculated as $2^{[C_T(input) - C_T(ChIP)]}$.

Molecular Pharmacology Fast Forward. Published on September 29, 2017 as DOI: 10.1124/mol.117.110379
This article has not been copyedited and formatted. The final version may differ from this version.

2.10 Animal studies

All animal studies adhered to standard operating procedures, animal ethics approval from the Animal Welfare Committee under IACUC guidelines, and conformed to good scientific practice.

2.11 Compound formulation in animal studies

RVX-297 was dosed orally for all animal studies, and was prepared in formulation EA006 as described by Jahagirdar *et al.* (Jahagirdar et al., 2014). The concentration of test compound in each preparation was verified by LC/MS/MS.

2.12 LPS induced endotoxemic mouse model

Endotoxemia studies in mice were performed at Aravasc (Sunnyvale, CA). Eight week old male C57Bl/6 mice (Charles River or Harlan Laboratories) received LPS (Sigma, St. Louis, MO) by intraperitoneal injection. RVX-297 was administered orally at 75 mg/kg 4 hours before and again at the time of stimulation with an amount of LPS producing optimal response. For serum cytokine determinations, animals received 5 µg of LPS. Serum levels of IL-6, IL-17, and interferon-γ (IFNγ) were determined by ELISA (R&D Systems Inc., Minneapolis, MN) 4 hours post-LPS. Multi-analyte profiling of serum was performed as outlined in the Supplemental section. Changes in gene expression, which precede changes in circulating protein levels, were measured in the spleen by real-time PCR as above except 3 hours after receiving 10 µg of LPS.

Molecular Pharmacology Fast Forward. Published on September 29, 2017 as DOI: 10.1124/mol.117.110379
This article has not been copyedited and formatted. The final version may differ from this version.

2.13 Rat collagen-induced arthritis (rCIA)

rCIA studies were performed at Aravasc (Sunnyvale, CA). Female Lewis rats (Charles River) were 6-8 weeks old and weighed approximately 150 grams. Bovine type II collagen (Chondrex Inc., Redmond, WA) was emulsified with incomplete Freund's adjuvant (IFA). Rats were immunized by intradermal injection at the sacro-lumbar region and base of the tail, and a booster was provided on day 7. Beginning on day 11 (arthritis phase), RVX-297 was administered orally twice per day (b.i.d.) for 6 days at 25, 50, and 75 mg/kg/dose. Body weight was tracked, and ankle diameter was monitored via caliper measurements. Systemic plasma exposure of RVX-297 was determined 1 day prior to the end of the study for pharmacokinetic / pharmacodynamic analysis (see Supplemental section). Histopathology of the ankle and knee (in the right paws – see Supplemental section), gene expression and cytokine levels in the ankle (left paws) were evaluated at the end of the study.

2.14 Mouse collagen induced arthritis

See Supplemental section.

2.15 Mouse collagen antibody induced arthritis (mCAIA)

mCAIA studies were performed at Aravasc (Sunnyvale, CA), and conducted as previously described (Khachigian, 2006)**.** Briefly, female BALB/cAnNHsd mice (Harlan Labs) weighing approximately 18 grams were injected intravenous with 2.5 mg/mouse of a cocktail containing four arthritogenic monoclonal antibodies to collagen-II (MD Bioproducts, St. Paul, MN). After 24 hours, mice received 25 µg of LPS (Sigma, St.

Molecular Pharmacology Fast Forward. Published on September 29, 2017 as DOI: 10.1124/mol.117.110379
This article has not been copyedited and formatted. The final version may differ from this version.

Louis, MO) by intraperitoneal injection to enhance the inflammatory response. Arthritis symptoms developed 24-48 hours later. Twice per day oral administration of RVX-297 (150 mg/kg) or dexamethasone, an anti-inflammatory corticosteroid (0.5 mg/kg), was initiated 30 hours following LPS and continued for 9 days during the arthritis phase. Efficacy evaluation was based on body weight, clinical arthritis scores (all 4 paws), combined hind paw weights, and histologic assessment of fore paws, hind paws, and knees (see Supplemental section).

2.16 Murine experimental autoimmune encephalomyelitis (EAE)

EAE studies were performed as outlined previously (Bittner et al., 2014; Thakker et al., 2007) at Hooke Laboratories Inc. (Lawrence, MA). This model of autoimmunity was used in both therapeutic and preventative regimens. EAE was induced in female C57Bl/6 mice of 18-23 grams (Taconic Farms) by immunization with myelin oligodendrocyte glycoprotein peptide 35-55 (MOG_{35-55}) in complete Freund's adjuvant (CFA). Two hours and 24 hours after immunization, pertussis toxin was administered by intraperitoneal injection. Compounds were delivered by oral gavage at 75 and 125 mg/kg twice per day (b.i.d.) for RVX-297 or 0.5 mg/kg once per day (q.d.) for FTY720 for 18 days once disease was established (at the first sign of EAE) in a therapeutic regimen, or for 27 days immediately after MOG immunization in a preventative regimen. Therapeutically, RVX-297 was not well tolerated at 125 mg/kg, and was adjusted to 100 mg/kg b.i.d. on day 10 of treatment. Vehicle and RVX-297 75 mg/kg treatment cohorts were comprised of 10 mice, while the RVX-297 150 mg/kg treatment cohort had 9 mice. EAE development and clinical score were evaluated based on clinical manifestations

Molecular Pharmacology Fast Forward. Published on September 29, 2017 as DOI: 10.1124/mol.117.110379
This article has not been copyedited and formatted. The final version may differ from this version.

published by Bittner *et al.* (Bittner et al., 2014). The mean maximum clinical score (MMS) and body weight were tracked. Spinal cords were collected at the end of the treatment period for gene expression analysis and examination of infiltrating cells by flow cytometry as outlined below. Histological assessment of inflammatory foci, apoptotic cells, and demyelination in the cervical, thoracic, and lumbar regions of the spinal cord were performed by Hooke Laboratories (hookelabs.com) using the protocol of Marusic *et al.* (Marusic et al., 2008) by an experienced observer blinded to the treatment group.

2.17 *Ex vivo* assessment of EAE mice

2.17.1 Lymphocytes: Lymphocytes isolated from inguinal and axilar nodes of EAE mice that had been treated with vehicle or RVX-297 for 11 days were cultured for 72 hours in the presence of MOG_{35-50}. Levels of secreted cytokines in cell supernatants were determined through cytometric bead assays.

2.17.2 CNS infiltrating cells: Following perfusion with PBS, cells from brain and spinal cord tissue were isolated by density gradient centrifugation. Isolated cells were cultured with PMA (50 ng/mL), ionomycin (0.5 µg/mL) and brefeldin (1 µg/mL) for 4-5 hours before analysis of the cells by flow cytometry as previously described (Bandukwala et al., 2011).

2.18 Statistical analysis

Student's t-test (two-tailed, unpaired) was used to evaluate differences between control groups and a single test treatment group. When multiple test treatments were

Molecular Pharmacology Fast Forward. Published on September 29, 2017 as DOI: 10.1124/mol.117.110379
This article has not been copyedited and formatted. The final version may differ from this version.

employed, a one-way ANOVA followed by Tukey's Multiple Comparison Test was used. Variance is shown as standard deviation in figures and tables.

3 RESULTS:

3.1 RVX-297 decreases proinflammatory gene expression in multiple cell types *in vitro*

The effect of RVX-297 on gene expression was evaluated in several immune cell types involved in autoimmunity and inflammation. IL-6 is an acute phase inflammatory cytokine secreted by a variety of cell types including macrophages, T-cells, B-cells, and fibroblasts; its transcription and secretion are induced rapidly following stimulation with LPS or IL-1β. RVX-297 suppressed IL-6 gene induction in human U937 macrophages, mouse primary B-cells isolated from the spleen, mouse BMDMs (Table 1), and THP-1 monocytes (data not shown) in a dose dependent manner. IL-1β is another proinflammatory cytokine linked to autoimmune disorders that is expressed in activated monocytes and macrophages (Dinarello, 2009). In LPS stimulated mouse BMDMs, IL-1β expression was repressed by RVX-297, demonstrating suppressive effects on multiple inflammatory mediators (Table 1). A downstream target of IL-6, monocyte chemotactic protein 1 (MCP1), was examined in human PBMCs. MCP1 is a chemokine that regulates migration and infiltration of monocytes and macrophages at sites of injury or infection (Carr et al., 1994). Although MCP1 gene expression is potently induced by IL-6 (Biswas et al., 1998), RVX-297 inhibited MCP1 expression in unstimulated human PBMCs (Table 1). This suggests RVX-297 downregulates expression of inflammatory

Molecular Pharmacology Fast Forward. Published on September 29, 2017 as DOI: 10.1124/mol.117.110379
This article has not been copyedited and formatted. The final version may differ from this version.

mediators independent from suppression of IL-6. PBMCs were also used as a source of T-cells. When PBMCs were stimulated with the T-cell receptor antibody OKT3, IL-17 mRNA was induced, indicating activation of T_H17 cells. RVX-297 inhibited antigen stimulation of T-cells and induction of IL-17 expression (Table 1). IL-6 and IL-17 are critical factors in progression of autoimmunity, and downregulation of these cytokines suggests BETi can impact multiple processes contributing to inflammation.

3.2 RVX-297 decreases proinflammatory gene expression in synovial fibroblasts isolated from patients with rheumatoid arthritis

RVX-297 treatment of synovial fibroblasts, isolated from the knee fluid of rheumatoid arthritis (RA) patients, repressed inflammatory gene expression. Resident synovial fibroblasts contribute significantly to the perpetuation of RA, and may even play a role in its initiation (Lefevre et al., 2015). TNFα treatment induced IL-6 gene expression in human synovial fibroblasts, an effect countered by RVX-297 in a dose dependent manner (Figure 1A). Consistent with our result, the pan-BETi JQ1 and BRD4 siRNA have both been reported to suppress IL-6 protein secretion from TNFα-stimulated human synovial fibroblasts (Zhang et al., 2015). Similarly, expression of another inflammatory marker, vascular cell adhesion protein 1 (VCAM-1), was also induced with TNFα treatment, which was countered by RVX-297 (Figure 1B). These data show that RVX-297 can modulate the inflammatory response of resident synovial fibroblasts whose activity is dysregulated in RA.

Molecular Pharmacology Fast Forward. Published on September 29, 2017 as DOI: 10.1124/mol.117.110379
This article has not been copyedited and formatted. The final version may differ from this version.

3.3 Mechanism of BETi suppression of proinflammatory gene expression

RVX-297 and pan-BETis (JQ1 and I-BET762) were all found to inhibit inflammation-induced gene expression in primary mouse BMDMs (Figure 2A). LPS stimulation induced IL-6 gene expression as expected (Nicodeme et al., 2010), and this induction was inhibited by RVX-297 in a dose dependent manner (Table 1 and Figure 2A). Both JQ1 (Filippakopoulos et al., 2010) and I-BET762 (Nicodeme et al., 2010), pan-BETi with chemical scaffolds distinct from RVX-297, also inhibited LPS-induced IL-6 gene expression. Upregulation of IL-1β and TNFα gene expression was also opposed by all three BETi compounds (RVX-297, JQ1 and I-BET762; data not shown). Thus, the induction of proinflammatory cytokines IL-6, IL-1β, and TNFα can be blocked by pharmacological inhibition of BET bromodomains, the mutual targets of BETi with different chemical scaffolds.

Chromatin immunoprecipitation (ChIP) studies revealed that RVX-297 interferes with BET protein binding to inflammatory gene promoters. As shown in Figure 2B, LPS treatment led to increased association of BRD2, 3, and 4 at the promoters of the BETi-sensitive genes IL-6, IL-1β (genes downregulated by BETi) and the BETi-insensitive gene NF-κBia (Nicodeme et al., 2010). RVX-297 reduced binding of BRD3 and BRD4, but not BRD2, to the IL-6 promoter (Figure 2B), in agreement with reduced expression of the corresponding mRNA (Table 1). RVX-297 also reduced the abundance of BRD4 on the IL-1β promoter, again in line with BETi sensitive gene expression (Table 1). However, BET protein abundance on the NF-κBia promoter was unaffected by RVX-297 BETi treatment, consistent with its reported insensitivity to BETi (Nicodeme et al., 2010).

Molecular Pharmacology Fast Forward. Published on September 29, 2017 as DOI: 10.1124/mol.117.110379
This article has not been copyedited and formatted. The final version may differ from this version.

Site specific alterations in BET protein abundance induced by BETi imply that results of the ChIP assays were not a consequence of globally altered chromatin structure.

BET proteins, in particular BRD4, have been reported to regulate the activity of RNA polymerase II (RNA polII) through recruitment of P-TEFb to activate transcription (Itzen et al., 2014; Yang et al., 2005). The active form of RNA polymerase II is phosphorylated on serine 2 (RNA polII P-Ser2), and its abundance on a gene is related to levels of transcription (Reviewed in (Phatnani and Greenleaf, 2006)). RVX-297 treatment reduced the amount of RNA polII P-Ser2 on the IL-6 and IL-1β promoters, but not NF-κBia (Figure 2B), consistent with reduced transcription of IL-6 and IL-1β (Table 1). There was no change in the level of acetylated histone H4 on the IL-6 promoter (data not shown), suggesting that BETi promotes displacement of BET proteins from chromatin without altering the associated histone acetylation. Cumulatively, our results indicate that the RVX-297 mediated reduction in IL-6 and IL-1β gene expression can be explained by displacement of BET proteins from acetylated histones, which disrupts the recruitment of transcriptionally active RNA polII to the promoter of BET sensitive genes. In this system, RVX-297 effects on abundance of BRD3 and 4 on the gene promoter were more predictive of transcription levels than was the abundance of BRD2.

3.4 RVX-297 suppresses cytokine production in LPS treated mice

Endotoxin injection has been widely used to study the acute inflammatory response; here we show that RVX-297 delivered 3-4 hours prior, and again at the time of stimulation, reduced both cytokine production and gene expression in LPS stimulated

Molecular Pharmacology Fast Forward. Published on September 29, 2017 as DOI: 10.1124/mol.117.110379
This article has not been copyedited and formatted. The final version may differ from this version.

endotoxemic mice. Circulating levels of LPS-induced IL-6, IL-17, and IFNγ were lower in the serum of RVX-297 treated mice compared to vehicle treated controls (Figure 3A). In concordance, IL-6 and IL-17 gene expression measured in the spleen isolated from LPS stimulated endotoxemic mice were also decreased (Figure 3B). Multianalyte profiling (MAP) analysis of serum from LPS stimulated endotoxemic mice demonstrated lower levels of numerous circulating cytokines, chemokines and adhesion molecules following RVX-297 treatment, including GM-CSF, MCP-1, MCP-5, IL-2, TNFα, and RANTES (Supplemental Table 1). These results confirm that RVX-297 has broad and rapid anti-inflammatory effects in a mouse model of endotoxemia.

3.5 RVX-297 inhibits progression of pathology in the rat collagen-induced arthritis model (rCIA)

Analysis of anti-inflammatory properties of RVX-297 was extended into animal models of autoimmunity. Collagen-induced arthritis is a commonly used rodent model of human RA (Williams, 2004). In the rat collagen-induced arthritis model (rCIA), collagen injections caused a significant increase in rat ankle diameter that developed over time in vehicle treated arthritic animals as expected (Figure 4A). This increase in ankle diameter was attenuated by RVX-297 treatment, with differences apparent at Day 2 for 50 and 75 mg/kg RVX-297 (ANOVA, Tukey, $p<0.05$), and at all doses of RVX-297 in the following days (ANOVA, Tukey, $p<0.01$ for 25 mg/kg and $p<0.001$ for 50 and 75 mg/kg doses; Figure 4A). In fact, ankle diameter did not differ significantly between the RVX-297 treatment groups and naïve animals. RVX-297 also dramatically reduced synovitis, cartilage damage, pannus formation, and bone resorption in the ankle and knee joint,

Molecular Pharmacology Fast Forward. Published on September 29, 2017 as DOI: 10.1124/mol.117.110379
This article has not been copyedited and formatted. The final version may differ from this version.

which was readily observed in Toluidine blue stained sections (Figure 4B). Pharmacokinetic / pharmacodynamic (PK/PD) analysis of ankle diameter and total ankle or knee histopathology showed that effects of RVX-297 reached a maximum at approximately 50 mg/kg b.i.d. (Table 2). This near-maximal PD response corresponds to a RVX-297 systemic exposure (AUC_{0-12}) of approximately 50,000 hr*ng/mL, which produced a clear and pronounced anti-inflammatory effect on all of the efficacy parameters assessed.

In the rCIA model, RVX-297 treatment also had a substantial impact on cytokine gene expression; IL-1β, RANKL, MMP3, and MMP13 expression were all significantly decreased in the ankle joints of arthritic rats following RVX-297 treatment at 75 mg/kg b.i.d. versus vehicle treated arthritic controls (Table 3; Student's t-test). In addition, IL-6 and VCAM-1 protein levels were significantly lower in the ankles of arthritic rats treated with RVX-297 versus vehicle (Table 3; Student's t-test). Further, MAP analysis demonstrated that additional protein markers of inflammation were also reduced in the ankle joint of RVX-297 treated animals (data not shown). Together, RVX-297 BETi had suppressive effects on the production of cytokines, adhesion molecules, and inflammatory factors, culminating in substantially reduced pathology in the rCIA model.

3.6 RVX-297 inhibits progression of pathology in the mouse collagen-induced arthritis model (mCIA)

The ability of RVX-297 to counter autoimmune disease progression was further characterized and confirmed in the mouse collagen-induced arthritis model (Inglis et al.,

Molecular Pharmacology Fast Forward. Published on September 29, 2017 as DOI: 10.1124/mol.117.110379
This article has not been copyedited and formatted. The final version may differ from this version.

2007). Collagen injections increased clinical arthritis score (CAS) as expected (Supplemental Figure 1A). Notably, RVX-297 at both 75 and 150 mg/kg and the positive control dexamethasone all prevented significant increases in CAS compared to the arthritic vehicle treated cohort from day 2 forward (Supplemental Figure 1A, ANOVA, Tukey). Effects of RVX-297 were dose dependent. Effects of dexamethasone and RVX-297 150 mg/kg were so profound that CAS was not distinguishable from naïve animals from day 3 on (ANOVA, Tukey). Similar to rCIA, histopathology scores in all paws, knee, and six-joint mean were significantly reduced with RVX-297 or dexamethasone compared to vehicle treated arthritic controls (Table 4; Student's t-test). In addition, significantly lower anti-collagen II IgG serum levels were measured in RVX-297 150 mg/kg treated mice compared to vehicle treated controls (Supplemental Figure 1B; ANOVA, Tukey). In fact, anti-collagen II IgG levels were statistically indistinguishable between the naïve cohort and RVX-297 150 mg/kg treated mice. Lower levels of anti-collagen II IgG indicate that RVX-297 inhibited B-cell activation and antibody production to moderate the response to collagen injection. Thus, RVX-297 ameliorates clinical arthritis scores, histopathology scores, and serum IgG levels in the mouse collagen-induced arthritis model.

3.7 RVX-297 inhibits pathology in the mouse collagen antibody-induced arthritis model (mCAIA)

The mCAIA model offers a distinct advantage over CIA as arthritic pathology develops in the absence of adjuvants (CFA or IFA). Collagen antibody injections caused a significant increase in CAS that developed with time in vehicle treated arthritic mice

Molecular Pharmacology Fast Forward. Published on September 29, 2017 as DOI: 10.1124/mol.117.110379
This article has not been copyedited and formatted. The final version may differ from this version.

compared to naïve (Figure 5; ANOVA, Tukey, $p<0.001$ from day 4 on), an observation analogous to the CIA models. Treatment was initiated after disease symptoms were established. RVX-297 prevented progression of clinical manifestations in this model by day 5, as indicated through CAS (Figure 5 ANOVA, Tukey vs vehicle). Dexamethasone, the positive control, restored CAS in CAIA mice to that of naïve animals (Figure 5; ANOVA, Tukey). Histopathology scores were also significantly reduced by RVX-297 compared to vehicle treated controls in both CIA and CAIA mice (Table 4; Student's t-test). Thus, RVX-297 and dexamethasone both produced clear and significant beneficial effects on the clinical parameters and histology associated with collagen antibody induced arthritis in mice. In all, the three autoimmune arthritis models presented here show that BET proteins play a principal role in the development and maintenance of pathology mimicking arthritis by contributing to the processes of inflammation, cartilage destruction, bone resorption, and production of antibodies underlying the autoimmune process. RVX-297, a BETi, can ameliorate arthritis symptoms through downregulation of factors derived from multiple contributing cell types that propagate or promote the disorder.

3.8 RVX-297 diminishes experimental autoimmune encephalomyelitis (EAE) pathology

Evaluation of RVX-297 treatment was extended to the EAE mouse model, a T-cell-mediated autoimmune model that shares many clinical and histopathological features with human MS. FTY720 (fingolimod), an approved drug for MS that is efficacious in the mouse EAE model (Kataoka et al., 2005), was used as a comparator treatment with a

Molecular Pharmacology Fast Forward. Published on September 29, 2017 as DOI: 10.1124/mol.117.110379
This article has not been copyedited and formatted. The final version may differ from this version.

mechanism of action distinct from BETi. RVX-297 or FTY720 treatment was initiated concurrent with induction of disease in a prevention model (Figure 6A), or after establishment of EAE in a therapeutic regimen (Figure 6B). The impact of treatment on EAE clinical scores (Figure 6C & D), the percent change in body weight (Figure 6E & F), and EAE dependent changes in spinal cord histology (Figure 6G & H; Table 5) were all assessed.

Within the prevention model, EAE clinical score began to increase significantly from baseline around day 15 post immunization (Figure 6C), which was suppressed remarkably by RVX-297 or FTY720 (ANOVA, Tukey, $p<0.05$ day 15 on). In the therapeutic regimen, RVX-297 countered the increase in EAE clinical scores in a dose dependent manner (Figure 6D ANOVA, Tukey, $p<0.05$ by day 2 on for RVX-297 125 mg/kg, day 9, 12, 13 & 14 for RVX-297 75 mg/kg and by day 4 on for FTY720). RVX-297 had a similar impact on clinical scores as FTY720, a MS therapeutic, in both the prevention and the therapeutic regimens.

Weight loss is a widely recognized symptom of EAE onset (Emerson et al., 2009). Here, body weight of the vehicle treated cohort began to deviate significantly from naïve animals by day 17 post immunization in the prevention study (Figure 6E; ANOVA, Tukey) and by day 13 in the therapeutic study (Figure 6F; ANOVA, Tukey). RVX-297 75 mg/kg and FTY720 both prevented substantial losses in body weight induced by EAE (Figure 6E; ANOVA, Tukey). RVX-297 at 125 mg/kg accelerated weight loss, as it was not well tolerated. Dose was adjusted to 100 mg/kg b.i.d. on day 10, and weight

Molecular Pharmacology Fast Forward. Published on September 29, 2017 as DOI: 10.1124/mol.117.110379
This article has not been copyedited and formatted. The final version may differ from this version.

recovery was apparent by day 17. Statistically, the weights of the RVX-297 100 mg/kg cohort were indistinguishable from the naïve, RVX-297 75 mg/kg, and FTY720 cohorts on days 20-24 (Figure 6E; ANOVA, Tukey). Our results demonstrate that RVX-297 and FTY720 treatments had clear and sustained effects on outward manifestations of EAE in both preventative and therapeutic regimens.

Histopathological examination of spinal cords revealed that vehicle treated mice had prominent hallmarks of EAE pathology (Figure 6G and H; left panels). Inflammatory foci were large, coalescing, and present around blood vessels in the leptomeninges as well as deep in the white matter. Demyelination was prevalent in all spinal cord sections and large numbers of apoptotic cells were apparent. Strikingly, mice treated with RVX-297 in the prophylactic protocol had no histological signs of EAE in the spinal cord, no inflammatory foci, no demyelination, no apoptotic cells in any of the histological sections, and were indistinguishable from naïve mice (Figure 6G, Table 5). The impact of RVX-297 on clinical scores (Figure 6C) is mirrored in the marked histological improvements observed with the preventative RVX-297 treatment of EAE mice. In the therapeutic regimen, microscopic evaluation showed that RVX-297 and FTY720 treated mice had significantly lower inflammation, as evidenced by a reduction in the number of inflammatory foci, an improvement in demyelination scores, and sparsity of apoptotic cells in the spinal cord compared to vehicle treated animals (Figure 6H, Table 5). Collectively, RVX-297 was effective in reducing disease severity and improving clinical parameters in mice when dosed after disease onset, and was highly efficacious in reducing EAE development when dosed concurrently with immunization.

Molecular Pharmacology Fast Forward. Published on September 29, 2017 as DOI: 10.1124/mol.117.110379
This article has not been copyedited and formatted. The final version may differ from this version.

Pro-inflammatory cytokines are important contributors to the establishment and progression of autoimmune diseases. The gene expression of critical inflammatory cytokines in the spinal cord was examined. mRNA levels of IL-6, IL-17, MCP-1, GM-CSF, and TNFα mRNAs were all significantly lower in RVX-297 treated EAE mice compared to vehicle treated controls (Figure 7; Student's t-test), suggesting that treatment prevented localized inflammation in the spinal cord. RVX-297 treatment also increased Hist2h2be gene expression in the spinal cord, a known BETi target engagement marker (Delmore et al., 2011; Mertz et al., 2011), more than 4-fold versus vehicle treated controls (data not shown). Myelin basic protein (MBP)-specific CD4(+) T-cells mediate EAE pathology by migrating from the periphery into the CNS (Furtado et al., 2008; O'Connor et al., 2008). Here, the percentage of CD4+ cells producing specific pro-inflammatory cytokines was quantified in the brain and spinal cord to determine the extent of infiltration into the CNS. RVX-297 significantly lowered the abundance of IL-6, GM-CSF, and IFNγ CD4+ cells, indicating a reduction in CNS infiltration (Figure 8). To examine cytokine production, lymphocytes were isolated from EAE mice that had been treated for 11 days with either vehicle or RVX-297, which were re-challenged with MOG_{35-55} *ex vivo*. Inflammatory cytokine secretion into the culture media (IL-17a, IL-6, TNFα, and IFNγ) was substantially reduced compared to lymphocytes isolated from vehicle treated controls (Table 6). Together, observations in EAE mice demonstrate that BETi modulates key mediators of inflammation that drive progression of autoimmunity from multiple contributing cell types, and can alleviate EAE pathology even after the onset of disease.

Molecular Pharmacology Fast Forward. Published on September 29, 2017 as DOI: 10.1124/mol.117.110379
This article has not been copyedited and formatted. The final version may differ from this version.

4 DISCUSSION:

Small molecule pan-BET inhibitors have been useful in delineating roles for BET bromodomains in inflammatory processes and autoimmune disorders (Barrett et al., 2014; Chen et al., 2016; Nicodeme et al., 2010; Zhang et al., 2015). Whereas most BET inhibitors in development have similar affinity for both (pan) BET protein bromodomains, RVX-297 is a novel, orally bioavailable BETi with selectivity for BD2 (Kharenko et al., 2016). Apabetalone is another BD2 selective BETi currently in clinical trials for cardiovascular disease (McLure et al., 2013); the anti-inflammatory properties of apabetalone have been demonstrated in a mouse model of atherosclerosis (Jahagirdar et al., 2014). To extend the understanding of RVX-297's anti-inflammatory properties, we examined the activity of RVX-297 *in vitro* and in five pre-clinical *in vivo* models of autoimmune pathology including the mLPS, rCIA, mCIA, mCAIA, and mEAE models. RVX-297 reduced the response to inflammatory stimuli in macrophages, B-cells, T-cells, and fibroblasts, consistent with displacement of BET proteins from chromatin. *In vivo*, RVX-297 drastically reduced disease symptoms in rodent models of endotoxemia and autoimmune disease. In addition, RVX-297 regulated inflammatory gene expression in disease contributing cell types.

Responses to inflammatory stimuli are complex. Activation of inflammatory gene expression involves epigenetic restructuring of chromatin and the associated regulatory elements to alter the transcriptome (Brown et al., 2014). Current evidence suggests that anti-inflammatory properties of BETi are mediated through the displacement of BET

Molecular Pharmacology Fast Forward. Published on September 29, 2017 as DOI: 10.1124/mol.117.110379
This article has not been copyedited and formatted. The final version may differ from this version.

proteins from acetylation marks on chromatin, disrupting the assembly of transcriptional machinery, and the subsequent expression of BET sensitive genes (Nicodeme et al., 2010). BETi also effectively suppress inflammatory responses mediated by NF-κB (Brown et al., 2014), a pro-inflammatory transcription factor and master regulator of inflammatory and immune responses (reviewed in (Baltimore, 2011; Smale, 2011)). For example, the NF-κB pathway is activated by LPS, and the pan-BETi I-BET762 has been shown to prevent or diminish incidence of death in mice given lethal doses of LPS (Nicodeme et al., 2010). This data indicates that modulation of BET protein activity can attenuate the cytokine storm associated with endotoxemic shock or sepsis. Genetic and chemical approaches have demonstrated the critical role of BRD2 and BRD4 in the regulation of inflammatory cytokine expression in macrophages (Belkina et al., 2013). In our study RVX-297 blunts LPS induced endotoxemia in mice, resulting in reduced serum cytokines, inflammatory markers (Figure 3A, Supplemental Table 1), and LPS induced splenic gene expression of IL-6 and IL-17 (Figure 3B). Our results are consistent with studies linking BETi with the suppression of exaggerated inflammatory responses tied to cytokine production and NF-κB activation (Belkina et al., 2013; Huang et al., 2009).

Because RVX-297 mediated the suppression of key factors that drive autoimmune disease in LPS treated mice, studies were extended to preclinical autoimmune models. Rodent models of RA provide insights into the perpetuation and treatment of pathogenic joint inflammation. The CIA and CAIA models are characterized by hallmarks of arthritis including measurable polyarticular inflammation, marked cartilage destruction in

Molecular Pharmacology Fast Forward. Published on September 29, 2017 as DOI: 10.1124/mol.117.110379
This article has not been copyedited and formatted. The final version may differ from this version.

association with pannus formation and mild to moderate bone resorption and periosteal bone proliferation (Bendele, 2001; Williams, 2004). In three arthritis models, disease indices were dramatically reduced in RVX-297 treated animals, resulting in maintenance of joint structure and integrity, likely arising from decreased production of cytokines and inflammatory mediators. The pan-BETi JQ1 is also efficacious in the mCIA model, stressing a role for BET proteins in the inflammatory response, production of autoantibodies, and joint damage arising in this model (Zhang et al., 2015). In addition, a fundamental role for IL-17 in CAIA model disease development has been demonstrated (Plum et al., 2009). The ability of RVX-297 to downregulate IL-17 production (Table 1, 6, Supplemental Table 1) may contribute to the efficacy of this compound.

T_H17 cells are fundamental in promoting human autoimmune disease, which is recapitulated in mouse models (Komiyama et al., 2006; Nakae et al., 2003). T-cells of both T_H1 and T_H17 lineage are involved in generating disease conditions in EAE (Kroenke et al., 2008). Cytokines IL-23, IL-6, and IL-17, critical for T_H1 and T_H17 differentiation and production of these T-cells, play a fundamental and non-redundant role in EAE progression (Thakker et al., 2007). Therefore, pharmacological suppression of these cytokines, or T_H17 differentiation, has therapeutic potential in T-cell-mediated autoimmune disorders. Further, neutralization of IL-17 through targeting of the protein or its receptor prevents the development of EAE (Hofstetter et al., 2005). Previous studies have demonstrated that JQ1 ameliorates EAE symptoms, and established that BET bromodomains are critical in the differentiation and function of T_H17 cells (Mele et al., 2013). RVX-297 suppressed EAE pathology when administered to mice either

Molecular Pharmacology Fast Forward. Published on September 29, 2017 as DOI: 10.1124/mol.117.110379
This article has not been copyedited and formatted. The final version may differ from this version.

prophylactically or therapeutically. In addition, the production of multiple cytokines *in vivo* (Figure 7) and *ex vivo* (Table 6) were suppressed by RVX-297. *In vivo* efficacy was comparable or superior to the S1P1 agonist, FTY720 (fingolimod), an approved therapeutic for treatment of MS. RVX-297 inhibits T_H1 and T_H17 responses, both of which play pivotal roles in development and progression of MS and other autoimmune indications. Additional analysis of cytokine production indicates RVX-297 affects multiple contributors to autoimmune pathology. Importantly, RVX-297 decreased CD4+ cells producing pro-inflammatory cytokines in the brain and spinal cord of EAE mice (Figure 8), indicating reduced infiltration of T-cells into the CNS. These results underscore the effects of BETi in the periphery to alleviate effects in the CNS (Tzartos et al., 2008). While RVX-297 was effective in reducing IL-17 producing T-cells in the CNS, more profound effects were reported with JQ1 (Mele et al., 2013). This variance may be due to differences in compound affinities for BET bromodomains. Results from this study and from other laboratories have shown that BET bromodomain inhibition protects mice from autoimmunity (Belkina et al., 2013; Mele et al., 2013; Zhang et al., 2015). Therefore, BETi holds promise for the treatment of autoimmunity, even after disease symptoms have been established.

A variety of pharmacological therapies have been approved for the treatment of autoimmune disorders. Antibodies that capture or neutralize key cytokines to promote immunosuppression are prevalent (reviewed in (Chan and Carter, 2010)). Because autoimmunity causing host tissue damage and anti-microbial immunity involve the same processes, infection is a concern due to the immunosuppressive nature of these drugs

Molecular Pharmacology Fast Forward. Published on September 29, 2017 as DOI: 10.1124/mol.117.110379
This article has not been copyedited and formatted. The final version may differ from this version.

(reviewed in (Caspi, 2008)). Therefore immunosuppressive therapies are often not well suited for long-term treatment. Of note, the BD2 selective compound apabetalone had no effect on the incidents of infestations or infections in a 6 month CVD patient clinical trial (Nicholls et al., 2016; Nikolic et al., 2015). This outcome may be a result of suppressing inflammatory processes to levels that do not entirely impair immune function, thereby avoiding risk of infection.

In contrast to targeting single entities in inflammatory or autoimmune pathways, BETi simultaneously downregulates multiple inflammatory processes. Concurrent targeting of contributors to inflammation from a variety of immune cell types sets BETi apart from current therapies that act on a single inflammatory component or process. Studies indicate BET protein BDs function cooperatively (Schroder et al., 2011, 2012). How BD1 is impacted, directly or indirectly, by BD2 selective inhibition requires further investigation. Our results suggest that BD2-selective BET inhibitors are sufficient to ameliorate autoimmune pathology and may dampen detrimental immune responses without adversely compromising immune function. Future studies will be required to determine if RVX-297 BETi is clinically effective in autoimmune conditions.

ACKNOWLEDGMENTS:

We are grateful to S. Wasiak, S. Stotz, and B. Rakai for stimulating discussions and critical review of the manuscript.

Molecular Pharmacology Fast Forward. Published on September 29, 2017 as DOI: 10.1124/mol.117.110379
This article has not been copyedited and formatted. The final version may differ from this version.

AUTHORSHIP CONTRIBUTIONS:

Participated in research design: Jahagirdar, Attwell, Marusic, Bendele, Shenoy, McLure, Hansen, Wagner, Young, Wong, Kulikowski

Conducted experiments: Attwell, Marusic, Bendele, Shenoy, Norek, Yu, Tobin

Performed data analysis: Jahagirdar, Attwell, Marusic, Bendele, Shenoy, McLure, Norek, Yu, Tobin,

Wrote or contributed to the writing of the manuscript: Gilham, Jahagirdar, Attwell,

REFERENCES:

Baltimore D (2011) NF-kappaB is 25. *Nature immunology* **12:** 683-685.

Bandukwala HS, Gagnon J, Togher S, Greenbaum JA, Lamperti ED, Parr NJ, Molesworth AM, Smithers N, Lee K, Witherington J, Tough DF, Prinjha RK, Peters B, and Rao A (2012) Selective inhibition of CD4+ T-cell cytokine production and autoimmunity by BET protein and c-Myc inhibitors. *Proc Natl Acad Sci U S A* **109:** 14532-14537.

Bandukwala HS, Wu Y, Feuerer M, Chen Y, Barboza B, Ghosh S, Stroud JC, Benoist C, Mathis D, Rao A, and Chen L (2011) Structure of a domain-swapped FOXP3 dimer on DNA and its function in regulatory T cells. *Immunity* **34:** 479-491.

Barrett E, Brothers S, Wahlestedt C, and Beurel E (2014) I-BET151 selectively regulates IL-6 production. *Biochim Biophys Acta* **1842:** 1549-1555.

Baumgart DC, and Carding SR (2007) Inflammatory bowel disease: cause and immunobiology. *Lancet* **369:** 1627-1640.

Belkina AC, Nikolajczyk BS, and Denis GV (2013) BET protein function is required for inflammation: Brd2 genetic disruption and BET inhibitor JQ1 impair mouse macrophage inflammatory responses. *J Immunol* **190:** 3670-3678.

Bendele A (2001) Animal models of rheumatoid arthritis. *Journal of musculoskeletal & neuronal interactions* **1:** 377-385.

Biswas P, Delfanti F, Bernasconi S, Mengozzi M, Cota M, Polentarutti N, Mantovani A, Lazzarin A, Sozzani S, and Poli G (1998) Interleukin-6 induces monocyte

chemotactic protein-1 in peripheral blood mononuclear cells and in the U937 cell line. *Blood* **91:** 258-265.

Bittner S, Afzali AM, Wiendl H, and Meuth SG (2014) Myelin oligodendrocyte glycoprotein (MOG35-55) induced experimental autoimmune encephalomyelitis (EAE) in C57BL/6 mice. *Journal of visualized experiments : JoVE***:** doi: 10.3791/51275.

Brown JD, Lin CY, Duan Q, Griffin G, Federation AJ, Paranal RM, Bair S, Newton G, Lichtman AH, Kung AL, Yang T, Wang H, Luscinskas FW, Croce KJ, Bradner JE, and Plutzky J (2014) NF-kappaB directs dynamic super enhancer formation in inflammation and atherogenesis. *Mol Cell* **56:** 219-231.

Carr MW, Roth SJ, Luther E, Rose SS, and Springer TA (1994) Monocyte chemoattractant protein 1 acts as a T-lymphocyte chemoattractant. *Proc Natl Acad Sci U S A* **91:** 3652-3656.

Caspi RR (2008) Immunotherapy of autoimmunity and cancer: the penalty for success. *Nature reviews Immunology* **8:** 970-976.

Chan AC, and Carter PJ (2010) Therapeutic antibodies for autoimmunity and inflammation. *Nature reviews Immunology* **10:** 301-316.

Chen K, Campfield BT, Wenzel SE, McAleer JP, Kreindler JL, Kurland G, Gopal R, Wang T, Chen W, Eddens T, Quinn KM, Myerburg MM, Horne WT, Lora JM, Albrecht BK, Pilewski JM, and Kolls JK (2016) Antiinflammatory effects of bromodomain and extraterminal domain inhibition in cystic fibrosis lung inflammation. *JCI insight* **1:** e87168.

Choy EH, and Panayi GS (2001) Cytokine pathways and joint inflammation in rheumatoid arthritis. *N Engl J Med* **344:** 907-916.

Delmore JE, Issa GC, Lemieux ME, Rahl PB, Shi J, Jacobs HM, Kastritis E, Gilpatrick T, Paranal RM, Qi J, Chesi M, Schinzel AC, McKeown MR, Heffernan TP, Vakoc CR, Bergsagel PL, Ghobrial IM, Richardson PG, Young RA, Hahn WC, Anderson KC, Kung AL, Bradner JE, and Mitsiades CS (2011) BET bromodomain inhibition as a therapeutic strategy to target c-Myc. *Cell* **146:** 904-917.

Dienz O, and Rincon M (2009) The effects of IL-6 on CD4 T cell responses. *Clin Immunol* **130:** 27-33.

Dinarello CA (2009) Immunological and inflammatory functions of the interleukin-1 family. *Annual review of immunology* **27:** 519-550.

Emerson MR, Gallagher RJ, Marquis JG, and LeVine SM (2009) Enhancing the ability of experimental autoimmune encephalomyelitis to serve as a more rigorous model of multiple sclerosis through refinement of the experimental design. *Comp Med* **59:** 112-128.

Filippakopoulos P, Picaud S, Mangos M, Keates T, Lambert JP, Barsyte-Lovejoy D, Felletar I, Volkmer R, Muller S, Pawson T, Gingras AC, Arrowsmith CH, and Knapp S (2012) Histone recognition and large-scale structural analysis of the human bromodomain family. *Cell* **149:** 214-231.

Filippakopoulos P, Qi J, Picaud S, Shen Y, Smith WB, Fedorov O, Morse EM, Keates T, Hickman TT, Felletar I, Philpott M, Munro S, McKeown MR, Wang Y, Christie AL, West N, Cameron MJ, Schwartz B, Heightman TD, La Thangue N, French CA, Wiest O, Kung AL, Knapp S, and Bradner JE (2010) Selective inhibition of BET bromodomains. *Nature* **468:** 1067-1073.

Furtado GC, Marcondes MC, Latkowski JA, Tsai J, Wensky A, and Lafaille JJ (2008) Swift entry of myelin-specific T lymphocytes into the central nervous system in spontaneous autoimmune encephalomyelitis. *J Immunol* **181:** 4648-4655.

Gacias M, Gerona-Navarro G, Plotnikov AN, Zhang G, Zeng L, Kaur J, Moy G, Rusinova E, Rodriguez Y, Matikainen B, Vincek A, Joshua J, Casaccia P, and Zhou MM (2014) Selective chemical modulation of gene transcription favors oligodendrocyte lineage progression. *Chemistry & biology* **21:** 841-854.

Gilham D, Wasiak S, Tsujikawa LM, Halliday C, Norek K, Patel RG, Kulikowski E, Johansson J, Sweeney M, and Wong NC (2016) RVX-208, a BET-inhibitor for treating atherosclerotic cardiovascular disease, raises ApoA-I/HDL and represses pathways that contribute to cardiovascular disease. *Atherosclerosis* **247:** 48-57.

Hansen HC (2011) Compounds for the prevention and treatment of cardiovascular diseases. *US Patent 8,053,440: Resverlogix Corp, Canada*.

Hofstetter HH, Ibrahim SM, Koczan D, Kruse N, Weishaupt A, Toyka KV, and Gold R (2005) Therapeutic efficacy of IL-17 neutralization in murine experimental autoimmune encephalomyelitis. *Cellular immunology* **237:** 123-130.

Huang B, Yang XD, Zhou MM, Ozato K, and Chen LF (2009) Brd4 coactivates transcriptional activation of NF-kappaB via specific binding to acetylated RelA. *Mol Cell Biol* **29:** 1375-1387.

Inglis JJ, Criado G, Medghalchi M, Andrews M, Sandison A, Feldmann M, and Williams RO (2007) Collagen-induced arthritis in C57BL/6 mice is associated with a robust and sustained T-cell response to type II collagen. *Arthritis Res Ther* **9:** R113.

Itzen F, Greifenberg AK, Bosken CA, and Geyer M (2014) Brd4 activates P-TEFb for RNA polymerase II CTD phosphorylation. *Nucleic Acids Res* **42:** 7577-7590.

Jahagirdar R, Zhang H, Azhar S, Tobin J, Attwell S, Yu R, Wu J, McLure KG, Hansen HC, Wagner GS, Young PR, Srivastava RA, Wong NC, and Johansson J (2014) A novel BET bromodomain inhibitor, RVX-208, shows reduction of atherosclerosis in hyperlipidemic ApoE deficient mice. *Atherosclerosis* **236:** 91-100.

Kataoka H, Sugahara K, Shimano K, Teshima K, Koyama M, Fukunari A, and Chiba K (2005) FTY720, sphingosine 1-phosphate receptor modulator, ameliorates experimental autoimmune encephalomyelitis by inhibition of T cell infiltration. *Cellular & molecular immunology* **2:** 439-448.

Khachigian LM (2006) Collagen antibody-induced arthritis. *Nat Protoc* **1:** 2512-2516.

Kharenko OA, Gesner EM, Patel RG, Norek K, White A, Fontano E, Suto RK, Young PR, McLure KG, and Hansen HC (2016) RVX-297- a novel BD2 selective inhibitor of BET bromodomains. *Biochemical and biophysical research communications* **477:** 62-67.

Kolls JK, and Linden A (2004) Interleukin-17 family members and inflammation. *Immunity* **21:** 467-476.

Komiyama Y, Nakae S, Matsuki T, Nambu A, Ishigame H, Kakuta S, Sudo K, and Iwakura Y (2006) IL-17 plays an important role in the development of experimental autoimmune encephalomyelitis. *J Immunol* **177:** 566-573.

Kroenke MA, Carlson TJ, Andjelkovic AV, and Segal BM (2008) IL-12- and IL-23-modulated T cells induce distinct types of EAE based on histology, CNS chemokine profile, and response to cytokine inhibition. *J Exp Med* **205:** 1535-1541.

Lefevre S, Meier FM, Neumann E, and Muller-Ladner U (2015) Role of synovial fibroblasts in rheumatoid arthritis. *Curr Pharm Des* **21:** 130-141.

Marusic S, Thakker P, Pelker JW, Stedman NL, Lee KL, McKew JC, Han L, Xu X, Wolf SF, Borey AJ, Cui J, Shen MW, Donahue F, Hassan-Zahraee M, Leach MW, Shimizu T, and Clark JD (2008) Blockade of cytosolic phospholipase A2 alpha prevents experimental autoimmune encephalomyelitis and diminishes development of Th1 and Th17 responses. *Journal of neuroimmunology* **204:** 29-37.

McCarthy KM, McDevit D, Andreucci A, Reeves R, and Nikolajczyk BS (2003) HMGA1 co-activates transcription in B cells through indirect association with DNA. *J Biol Chem* **278:** 42106-42114.

McLure KG, Gesner EM, Tsujikawa L, Kharenko OA, Attwell S, Campeau E, Wasiak S, Stein A, White A, Fontano E, Suto RK, Wong NC, Wagner GS, Hansen HC, and Young PR (2013) RVX-208, an Inducer of ApoA-I in Humans, Is a BET Bromodomain Antagonist. *PLoS One* **8:** e83190.

Mele DA, Salmeron A, Ghosh S, Huang HR, Bryant BM, and Lora JM (2013) BET bromodomain inhibition suppresses TH17-mediated pathology. *J Exp Med* **210:** 2181-2190.

Mertz JA, Conery AR, Bryant BM, Sandy P, Balasubramanian S, Mele DA, Bergeron L, and Sims RJ, 3rd (2011) Targeting MYC dependence in cancer by inhibiting BET bromodomains. *Proc Natl Acad Sci U S A* **108:** 16669-16674.

Nakae S, Nambu A, Sudo K, and Iwakura Y (2003) Suppression of immune induction of collagen-induced arthritis in IL-17-deficient mice. *J Immunol* **171:** 6173-6177.

Nicholls SJ, Puri R, Wolski K, Ballantyne CM, Barter PJ, Brewer HB, Kastelein JJ, Hu B, Uno K, Kataoka Y, Herrman JP, Merkely B, Borgman M, and Nissen SE (2016) Effect of the BET Protein Inhibitor, RVX-208, on Progression of Coronary Atherosclerosis: Results of the Phase 2b, Randomized, Double-Blind, Multicenter, ASSURE Trial. *Am J Cardiovasc Drugs* **16:** 55-65.

Nicodeme E, Jeffrey KL, Schaefer U, Beinke S, Dewell S, Chung CW, Chandwani R, Marazzi I, Wilson P, Coste H, White J, Kirilovsky J, Rice CM, Lora JM, Prinjha RK, Lee K, and Tarakhovsky A (2010) Suppression of inflammation by a synthetic histone mimic. *Nature* **468:** 1119-1123.

Nikolic D, Rizzo M, Mikhailidis DP, Wong NC, and Banach M (2015) An evaluation of RVX-208 for the treatment of atherosclerosis. *Expert opinion on investigational drugs* **24:** 1389-1398.

O'Connor RA, Prendergast CT, Sabatos CA, Lau CW, Leech MD, Wraith DC, and Anderton SM (2008) Cutting edge: Th1 cells facilitate the entry of Th17 cells to the central nervous system during experimental autoimmune encephalomyelitis. *J Immunol* **181:** 3750-3754.

Phatnani HP, and Greenleaf AL (2006) Phosphorylation and functions of the RNA polymerase II CTD. *Genes Dev* **20:** 2922-2936.

Picaud S, Wells C, Felletar I, Brotherton D, Martin S, Savitsky P, Diez-Dacal B, Philpott M, Bountra C, Lingard H, Fedorov O, Muller S, Brennan PE, Knapp S, and

Filippakopoulos P (2013) RVX-208, an inhibitor of BET transcriptional regulators with selectivity for the second bromodomain. *Proc Natl Acad Sci U S A* **110:** 19754-19759.

Plum SM, Park EJ, Strawn SJ, Moore EG, Sidor CF, and Fogler WE (2009) Disease modifying and antiangiogenic activity of 2-methoxyestradiol in a murine model of rheumatoid arthritis. *BMC musculoskeletal disorders* **10:** 46.

Schroder S, Cho S, Zeng L, Zhang Q, Kaehlcke K, Mak L, Lau J, Bisgrove D, Schnolzer M, Verdin E, Zhou MM, and Ott M (2011) Binding of the second bromodomain in Brd4 to tri-acetylated cyclin T1 and active dissociation of Hexim1 by the C-terminal P-TEFb-interacting domain in Brd4. *J Biol Chem* **287:** 1090-1099.

Schroder S, Cho S, Zeng L, Zhang Q, Kaehlcke K, Mak L, Lau J, Bisgrove D, Schnolzer M, Verdin E, Zhou MM, and Ott M (2012) Two-pronged binding with bromodomain-containing protein 4 liberates positive transcription elongation factor b from inactive ribonucleoprotein complexes. *J Biol Chem* **287:** 1090-1099.

Smale ST (2011) Hierarchies of NF-kappaB target-gene regulation. *Nature immunology* **12:** 689-694.

Thakker P, Leach MW, Kuang W, Benoit SE, Leonard JP, and Marusic S (2007) IL-23 is critical in the induction but not in the effector phase of experimental autoimmune encephalomyelitis. *J Immunol* **178:** 2589-2598.

Toniolo PA, Liu S, Yeh JE, Moraes-Vieira PM, Walker SR, Vafaizadeh V, Barbuto JA, and Frank DA (2015) Inhibiting STAT5 by the BET bromodomain inhibitor JQ1 disrupts human dendritic cell maturation. *J Immunol* **194:** 3180-3190.

Tzartos JS, Friese MA, Craner MJ, Palace J, Newcombe J, Esiri MM, and Fugger L (2008) Interleukin-17 production in central nervous system-infiltrating T cells and glial cells is associated with active disease in multiple sclerosis. *Am J Pathol* **172:** 146-155.

Wei G, Wei L, Zhu J, Zang C, Hu-Li J, Yao Z, Cui K, Kanno Y, Roh TY, Watford WT, Schones DE, Peng W, Sun HW, Paul WE, O'Shea JJ, and Zhao K (2009) Global mapping of H3K4me3 and H3K27me3 reveals specificity and plasticity in lineage fate determination of differentiating CD4+ T cells. *Immunity* **30:** 155-167.

Williams RO (2004) Collagen-induced arthritis as a model for rheumatoid arthritis. *Methods Mol Med* **98:** 207-216.

Yang Z, Yik JH, Chen R, He N, Jang MK, Ozato K, and Zhou Q (2005) Recruitment of P-TEFb for stimulation of transcriptional elongation by the bromodomain protein Brd4. *Molecular cell* **19:** 535-545.

Ye P, Rodriguez FH, Kanaly S, Stocking KL, Schurr J, Schwarzenberger P, Oliver P, Huang W, Zhang P, Zhang J, Shellito JE, Bagby GJ, Nelson S, Charrier K, Peschon JJ, and Kolls JK (2001) Requirement of interleukin 17 receptor signaling for lung CXC chemokine and granulocyte colony-stimulating factor expression, neutrophil recruitment, and host defense. *J Exp Med* **194:** 519-527.

Zhang QG, Qian J, and Zhu YC (2015) Targeting bromodomain-containing protein 4 (BRD4) benefits rheumatoid arthritis. *Immunol Lett* **166:** 103-108.

Molecular Pharmacology Fast Forward. Published on September 29, 2017 as DOI: 10.1124/mol.117.110379
This article has not been copyedited and formatted. The final version may differ from this version.

FOOTNOTES:

This research was funded by Resverlogix Corp. and did not receive any specific grant from funding agencies in the public, commercial, or not-for-profit sectors.

FIGURE LEGENDS:

Figure 1: RVX-297 Downregulates IL-6 and VCAM-1 gene expression in Synovial Fibroblasts from Patients with Rheumatoid Arthritis

Synovial fibroblasts isolated from fluid obtained from patients with rheumatoid arthritis were stimulated with TNFα and treated with RVX-297 for 24 hours. Gene expression was measured by real-time PCR for **(A)** IL-6 or **(B)** VCAM-1. Data are the mean ± standard deviation of independent triplicate samples. One-way ANOVA followed by Tukey's multiple comparison test was used to determine statistical significance compared to DMSO treated cells (***, $p<0.001$).

Figure 2: BET Bromodomains Regulate Macrophage Cytokine Gene Expression

A: Mouse bone marrow derived macrophages (BMDM) were stimulated with LPS and then treated with different concentrations of RVX-297 or pan-BETi with distinct chemical scaffolds (I-BET762 and JQ1) for 3 hours. Gene expression was assessed by real-time PCR. Each data point represents the mean ± standard deviation of independent triplicate samples. IC_{50} was 3.0, 0.2, and 0.5 μM for RVX-297, I-BET762 and JQ1 respectively.

Molecular Pharmacology Fast Forward. Published on September 29, 2017 as DOI: 10.1124/mol.117.110379
This article has not been copyedited and formatted. The final version may differ from this version.

B: Mouse BMDMs were stimulated with LPS and treated with 10 μM RVX-297 or 0.1% DMSO. Chromatin immunoprecipitation was performed for BRD2, 3, 4 or active RNA polymerase II (RNA polII P-Ser2), and their relative abundance on the promoter of the genes indicated were determined. IgG was used as a control. Data are representative of 2 independent experiments.

Figure 3: RVX-297 Suppresses LPS Induced Cytokine Production in Mice

RVX-297 (black bars) or vehicle (grey bars) was delivered to C57Bl/6 mice 4 hours before, and again when stimulated with LPS. **A:** Serum cytokine levels were determined by ELISA 4 hours post-LPS. **B:** Gene expression in the spleen was determined by real-time PCR 3 hours post-LPS. n=6-8 animals per group. Graphs show the mean ± standard deviation. Statistical significance was determined with a Student's t-test (*p<0.05, **p<0.01, ***p<0.001).

Figure 4: RVX-297 Prevents Swelling and Inflammation of the Ankle and Knee Joints in the Rat Collagen Induced Arthritis Model (rCIA)

rCIA disease progression was assessed in female Lewis rats receiving no treatment (naïve n=2), vehicle alone (n=7), or the indicated b.i.d. doses of RVX-297 (n=7 per group). Oral dosing began after arthritis symptoms were established; that time point was designated day 1. **A:** Changes in ankle diameter (mean ± standard deviation). Changes in ankle diameter were apparent by day 3 on in arthritis and arthritis+vehicle compared to naïve (ANOVA, Tukey, p<0.001). Change in ankle diameter of RVX-297 treated CIA rats varied significantly from the arthritis and arthritis+vehicle treatment cohorts starting

at day 2 for RVX-297 doses of 50 & 75 mg/kg and day 3 for RVX-297 at 25 mg/kg (ANOVA, Tukey; $p<0.05$).

B: RVX-297 treatment decreased inflammation in rCIA ankle and knee joints. Representative toluidine blue staining of an ankle and a knee joint following 7 days of treatment with vehicle or RVX-297 75 mg/kg. Areas of inflammation are marked with S, large arrows point to areas with cartilage damage, and small arrows point to areas of pannus formation.

Figure 5: RVX-297 Improves Clinical Arthritis Scores in the Mouse Collagen Antibody Induced Arthritis Model (mCAIA)

Oral RVX-297 b.i.d. dosing was initiated after establishment of CAIA in female BALB/cAnNHsd mice. Clinical arthritis scores (scored 0-5; www.bolderbiopath.com) are presented as the mean ± standard deviation (n=10 mice per group except naïve n=5). CAS rapidly increased following CAIA establishment (ANOVA, Tukey, $p<0.001$, arthritis+vehicle vs naïve from day 4 on). RVX-297 treatment significantly reduced the clinical arthritis score in CAIA mice vs vehicle by day 5 on (ANOVA, Tukey, $p<0.05$). Dexamethasone (dex) treatment suppressed increases in clinical arthritis score in CAIA mice (ANOVA, Tukey $p<0.05$ day 4 on vs vehicle. No significant difference vs naïve day 4 on).

Figure 6: RVX-297 Ameliorates Clinical Manifestations and Histopathology Associated with Mouse EAE in Both Prevention and Therapeutic Regimens

Molecular Pharmacology Fast Forward. Published on September 29, 2017 as DOI: 10.1124/mol.117.110379
This article has not been copyedited and formatted. The final version may differ from this version.

A and **B:** Prevention and Therapeutic study designs, respectively. In both studies mice were evaluated prior to initiation (day -1), and EAE was induced on day 0. **C:** RVX-297 and FTY720 both prevented the rise in EAE clinical score observed 14 days after EAE induction; data are the mean ± standard deviation. At day 15 the clinical scores for the RVX-297 125 mg/kg and FTY720 treatment groups differed significantly from the vehicle treated cohort (ANOVA, Tukey, $p<0.05$), and by day 16 for the RVX-297 75 mg/kg cohort. **D:** RVX-297 and FTY720 had a therapeutic effect on EAE clinical scores. Data are presented as the mean ± standard deviation. Beginning on day 2, RVX-297 125 mg/kg significantly decreased the EAE clinical score compared to vehicle (ANOVA, Tukey, $p<0.05$). By day 4 on, FTY720 effectively decreased the EAE clinical score compared to vehicle. RVX-297 75 mg/kg differed significantly from vehicle on days 9, 12-14 (ANOVA, Tukey, $p<0.05$). **E:** RVX-297 75 mg/kg and FTY720 prevented EAE associated weight loss. Comparison of percent change in body weight observed for the RVX-297 75 mg/kg, FTY720, and naïve cohorts revealed no significant differences (ANOVA, Tukey). **F:** RVX-297 and FTY720 treatments reduced EAE associated weight loss in the therapeutic regimen. RVX-297 125 mg/kg treatment reduced weight loss compared to vehicle treated controls on day 15 & 22 (ANOVA, Tukey, $p<0.05$). FTY720 and RVX-297 75 mg/kg reduced weight loss compared to vehicle on day 17 (ANOVA, Tukey, $p<0.05$). **G** and **H:** Areas of spinal cord demyelination were identified by Luxol fast blue staining (arrows; 100X magnification). In the representative specimens shown, it is apparent that RVX-297 treatment in both the preventative (G) and therapeutic (H) treatment regimens decreased demyelination compared to vehicle treatment.

Molecular Pharmacology Fast Forward. Published on September 29, 2017 as DOI: 10.1124/mol.117.110379
This article has not been copyedited and formatted. The final version may differ from this version.

Figure 7: RVX-297 Decreases Inflammatory Gene Expression in the Spinal Cord of EAE Mice

Inflammatory gene expression (IL-6, IL-17, MCP-1, GM-CSF, and TNFα) in spinal cords of EAE mice treated orally b.i.d. with vehicle or 100 mg/kg RVX-297 in the preventative regimen was determined by real-time PCR. Data are the mean of either 9 or 10 animals per group. Error bars represent standard deviation. Statistical significance was determined with a Student's t-test (*, $p<0.05$).

Figure 8: RVX-297 Prevents CD4+ Cell CNS Infiltration and Cytokine Production in EAE Mice

Activated CD4+ T-cells producing the indicated pro-inflammatory cytokines in the brain and spinal cord of EAE mice treated with vehicle or 100 mg/kg RVX-297 were isolated. The CD4+ T-cells were further stimulated with PMA, ionomycin and brefeldin for 4-5 hours, and then quantified by flow cytometry. Data are the mean percent reductions in cells from RVX-297 treated versus vehicle treated; n=6 mice per group. Error bars represent standard deviation. Statistical significance versus vehicle treated controls was determined with a Student's t-test (*, $p<0.05$).

Molecular Pharmacology Fast Forward. Published on September 29, 2017 as DOI: 10.1124/mol.117.110379
This article has not been copyedited and formatted. The final version may differ from this version.

TABLES:

Table 1: RVX-297 Reduces Gene Expression of Inflammatory Mediators *In Vitro*

mRNA	Cell System	Stimulant	RVX-297 IC_{50} (μM)
IL-6	Human U937	LPS	0.71 ± 0.07
MCP1	Human PBMC	none	0.4 ± 0.2
IL-17	Human PBMC	OKT3	1.3 ± 0.5
IL-6	Mouse B-cells	LPS & ionomycin	0.46 to 0.53
IL-6	Mouse BMDM	LPS	0.4 to 3.0
IL-1β	Mouse BMDM	LPS	2.1 to 23.6

Cells were treated with inflammatory stimuli and RVX-297 as described in Materials and Methods. Each data point in the dose response analysis was collected using biological triplicates. Gene expression was measured by real-time PCR, and IC_{50} values determined through nonlinear regression (normalized response and variable slope) using GraphPad Prism software version 5.04. Results are shown as mean ± standard deviation when replicated in at least 3 independent experiments or as the range from 2 independent experiments.

Table 2: RVX-297 Suppresses Histopathological Parameters in Rat Collagen-Induced Arthritis

Group	Dose (mg/kg b.i.d.)	Mean AUC Change in Ankle Diameter	% Inhibition in AUC Change in Ankle Diameter	% Reduction in Ankle Histopathology Score	% Reduction in Knee Histopathology Score	RVX-297 Plasma Exposure $AUC_{(0-12)}$ (hr*ng/mL)
Naïve	na	0.05	na	na	na	na
Vehicle	0	7.5 ± 1.4	na	0 ± 4.5%	0 ± 33%	na
RVX-297	25	2.6 ± 2.3	66	26 ± 25%	83 ± 30%	23,165
RVX-297	50	0.9 ± 1.8	89	64 ± 29%	86 ± 17%	52,145
RVX-297	75	0.7 ± 1.5	92	64 ± 20%	94 ± 10%	86,452

Efficacy of RVX-297 is shown for n=2 for naïve and n=8 for all other groups. Area under the curve (AUC), shown for change in ankle diameter (days * mm), is the sum of changes in ankle diameter relative to baseline versus plasma exposure of RVX-297 (hr*ng/mL). Histopathology in ankle or knee joints were scored based on polyarticular inflammation, cartilage destruction, pannus formation, and bone resorption as outlined at www.bolderbiopath.com. na=not applicable. All parameters for RVX-297 treated animals were significantly different from vehicle controls (Student's t-test or Wilcoxon's non-parametric test, $p<0.05$). Variability is shown as standard deviation.

Molecular Pharmacology Fast Forward. Published on September 29, 2017 as DOI: 10.1124/mol.117.110379
This article has not been copyedited and formatted. The final version may differ from this version.

Table 3: RVX-297 Decreases Cytokine Gene and Protein Levels in the Ankle of Rat Collagen-Induced Arthritis Model

Percent inhibition in RVX-297 treated rats versus vehicle treated			
% reduction in gene expression in ankles		% reduction in ankle joint protein	
IL-1β	77 ± 16% ***	IL-6	52 ± 28% *
MMP3	60 ± 21% ***	VCAM-1	33 ± 4% ***
MMP13	37 ± 16% ***		
RANKL	70 ± 6% ***		

Mean percent reduction in paw joint gene expression in the ankle (n=7) or protein levels (n=4) in rCIA treated with 75 mg/kg b.i.d. RVX-297 versus vehicle treated controls. Variability is shown as standard deviation. Statistical significance compared to the vehicle treated controls was determined using a Student's t-test (*p<0.05, ***p<0.001).

Molecular Pharmacology Fast Forward. Published on September 29, 2017 as DOI: 10.1124/mol.117.110379
This article has not been copyedited and formatted. The final version may differ from this version.

Table 4: RVX-297 Reduces Histopathology in Mouse Models of Arthritis

	Reduction in histopathology score (%)				
	mCIA			mCAIA	
	RVX-297 75 mg/kg	RVX-297 150 mg/kg	Dexamethasone 0.2 mg/kg	RVX-297 150 mg/kg	Dexamethasone 0.5 mg/kg
All paw	65 ± 19% ***	79 ± 20% ***	92 ± 12% ***	49 ± 50%	94 ± 19% ***
Knee	70 ± 32% ***	92 ± 13% ***	87 ± 21% ***	73 ± 13% *	100 ± 0% **
6-joint	66 ± 21% ***	83 ± 18% ***	91 ± 13% ***	nd	nd
3-joint	nd	nd	nd	56 ± 33% *	96 ± 13% ***

Histopathology was assessed and scored based on polyarticular inflammation, cartilage destruction, pannus formation, and bone resorption (outlined at www.bolderbiopath.com). Doses were delivered twice per day in 10 mice per group. Results are presented as percent reduction compared to vehicle treated mCIA or mCAIA controls, and variability presented as standard deviation. nd=not determined. Statistical significance compared to the vehicle treated controls was determined using a Student's t-test (*p<0.05, **p<0.01, ***p<0.001).

Molecular Pharmacology Fast Forward. Published on September 29, 2017 as DOI: 10.1124/mol.117.110379
This article has not been copyedited and formatted. The final version may differ from this version.

Table 5: RVX-297 and FTY720 Reduce Inflammation, Demyelination, and Apoptosis in the Spinal Cord of EAE Mice

Preventative Treatment Regimen						
Group Treatment	**Inflammatory Foci ± SD**	**p value**	**Demyelination (LFB) ± SD**	**p value**	**Apoptotic Cells ± SD**	**p value**
Naïve	0.0 ± 0.0	<0.0001	0.0 ± 0.0	<0.0001	0.0 ± 0.0	<0.0001
Vehicle	4.3 ± 3.2	na	1.6 ± 1.0	na	2.7 ± 2.5	na
FTY720 (3 mg/kg)	0.3 ± 1.0	<0.0001	0.0 ± 0.2	<0.0001	0.1 ± 0.4	<0.0001
RVX-297 (75 mg/kg)	1.5 ± 2.9	0.0004	0.1 ± 0.3	<0.0001	0.5 ± 0.9	<0.0001
RVX-297 (125 mg/kg)	0.1 ± 0.6	<0.0001	0.0 ± 0.0	<0.0001	0.0 ± 0.0	<0.0001
Therapeutic Treatment Regimen						
Naïve	0.0 ± 0.0	<0.0001	0.0 ± 0.0	<0.0001	0.0 ± 0.0	<0.0001
Vehicle	3.9 ± 2.4	na	1.6 ± 0.8	na	2.0 ± 1.8	na
FTY720 (3 mg/kg)	0.8 ± 0.9	<0.0001	0.8 ± 0.5	<0.0001	0.8 ± 0.9	0.002
RVX-297 (75 mg/kg)	1.7 ± 1.2	<0.0001	1.1 ± 0.8	0.02	0.5 ± 1.0	0.0002
RVX-297 (125 mg/kg)	1.6 ± 1.9	0.0001	0.9 ± 0.8	0.002	0.3 ± 0.6	<0.0001

Histology was assessed in the cervical, thoracic and lumbar regions of the spinal cord of EAE mice. Each parameter is presented as an average from these regions compared to vehicle treated disease controls. Student's t-test (p values presented in table) was used to determine significant differences compared to vehicle treated EAE mice (n=10 per group except naïve n=3). LFB=Luxol fast blue. na=not applicable.

Molecular Pharmacology Fast Forward. Published on September 29, 2017 as DOI: 10.1124/mol.117.110379
This article has not been copyedited and formatted. The final version may differ from this version.

Table 6: RVX-297 Decreases *Ex Vivo* Cytokine Production by Lymphocytes Isolated from EAE Mice

***Ex vivo* lymphocyte cytokine production: % Inhibition in cells from RVX-297 treated mice versus vehicle treated**			
Protein	**MOG (μg/mL)**		
	0.7	**2.2**	**6.7**
IL-17a	67 ± 9% **	80 ± 7% **	73 ± 11% ***
IL-6	37 ± 13%*	58 ± 12% **	64 ± 4% **
TNFα	50 ± 15% *	79 ± 4% **	79 ± 5% ***
IFNγ	93 ± 1% ^{NS}	99 ± 0% *	99 ± 0% ***

Lymphocytes were isolated from EAE mice treated with RVX-297 (n=3) or vehicle (n=3) for 11 days. Independent cultures established from each mouse were re-challenged with MOG_{35-55} for 72 hours and secreted cytokine levels determined through cytometric bead assays run in triplicate. Data represent the mean reduction in cytokines produced by cells from RVX-297 treated mice compared to cells from vehicle treated controls, and variability presented as standard deviation. Statistical differences were determined with a Student's t-test (NS = not significant, * $p<0.05$, ** $p<0.01$, *** $p<0.001$).

Figure 1A:

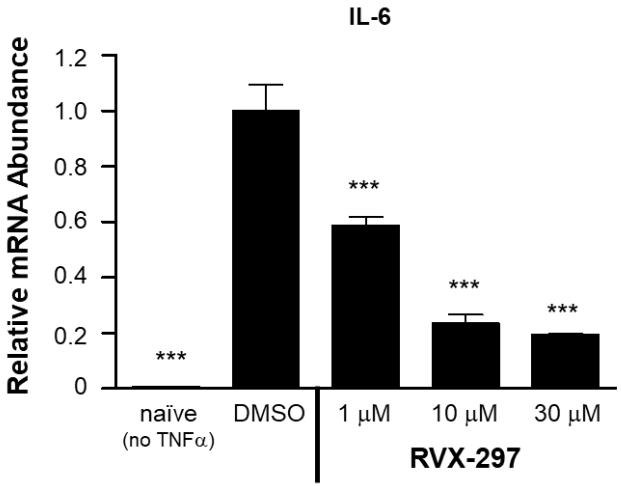

Figure 1B:

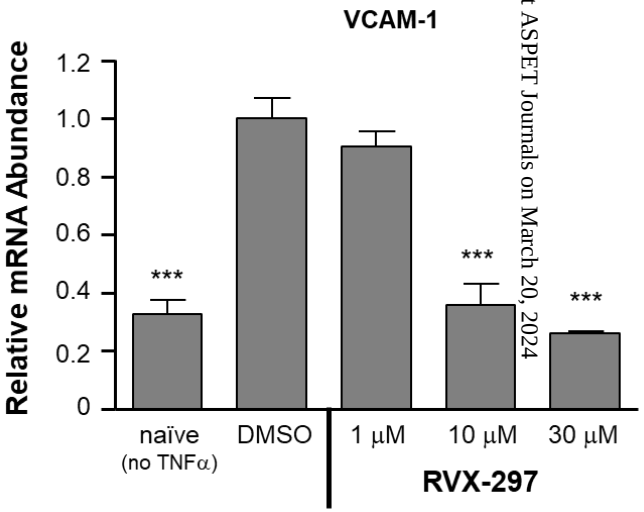

Figure 2A:

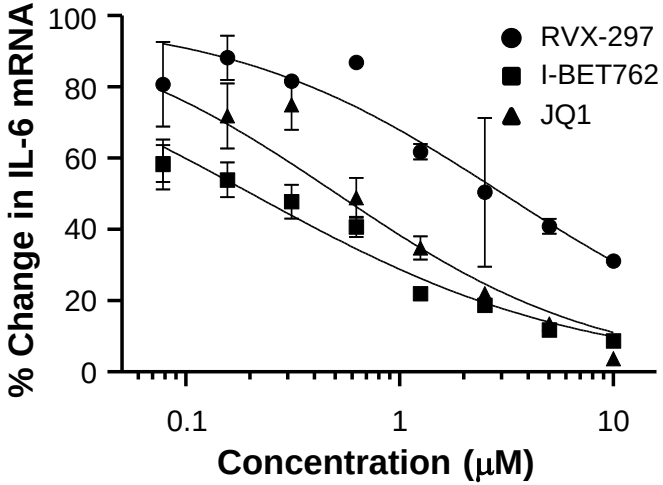

Figure 2B:

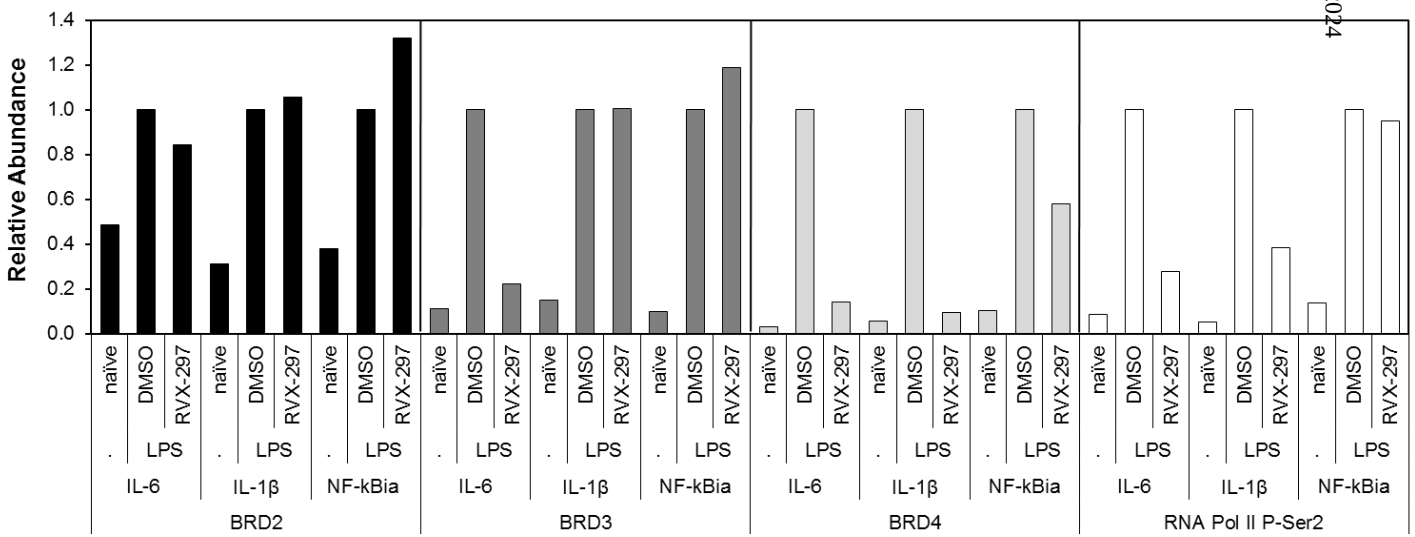

Figure 3A:

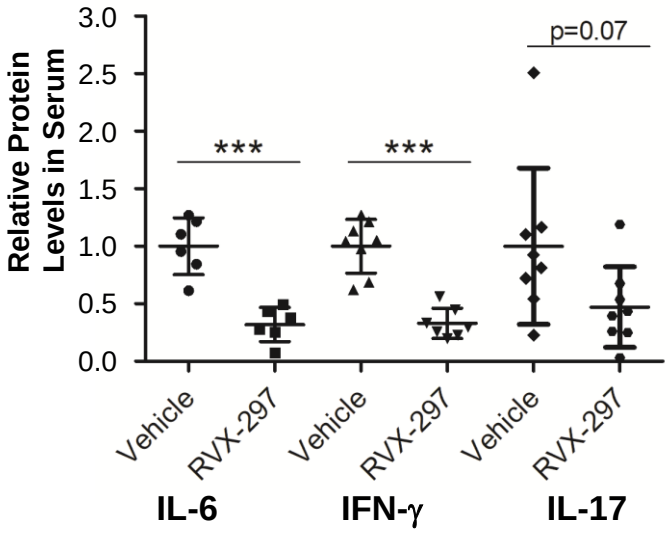

Figure 3B:

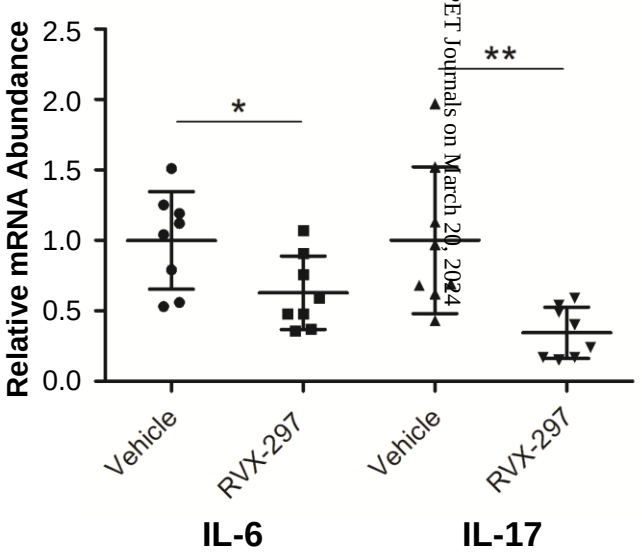

Figure 4A:

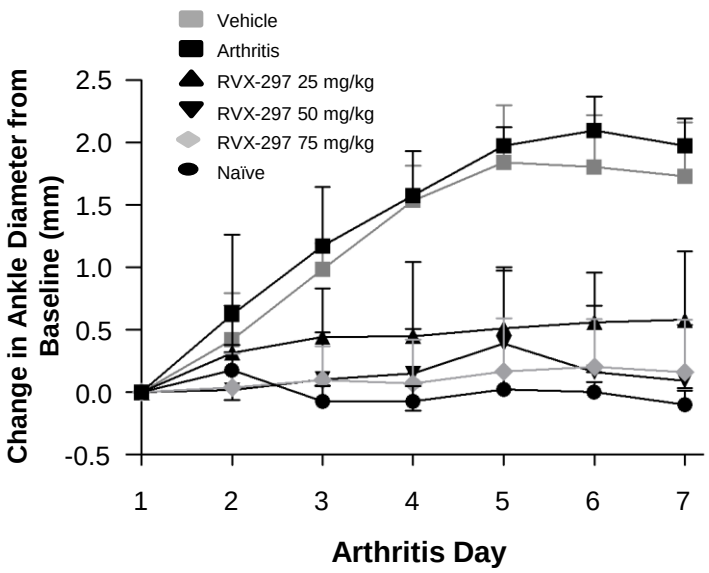

Figure 4B:

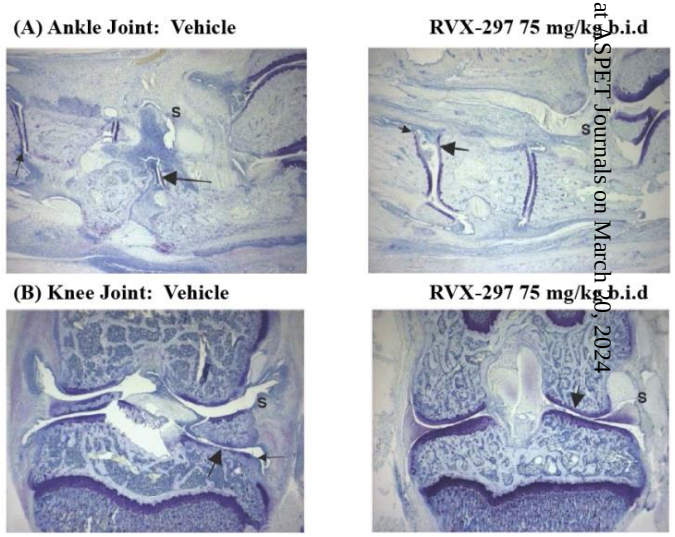

Figure 5:

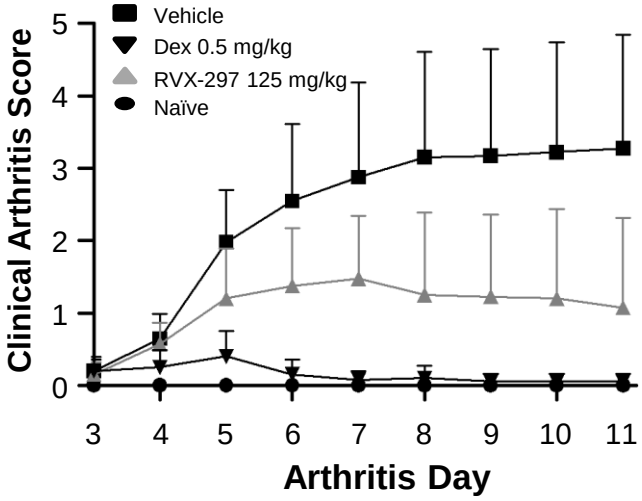

Figure 6A:

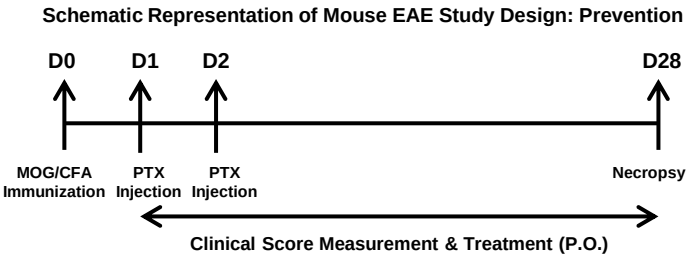

Figure 6B:

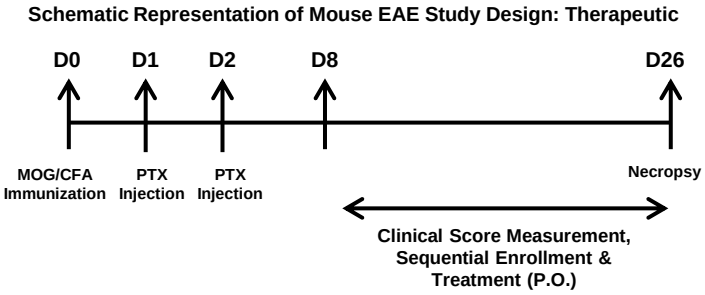

Figure 6C:

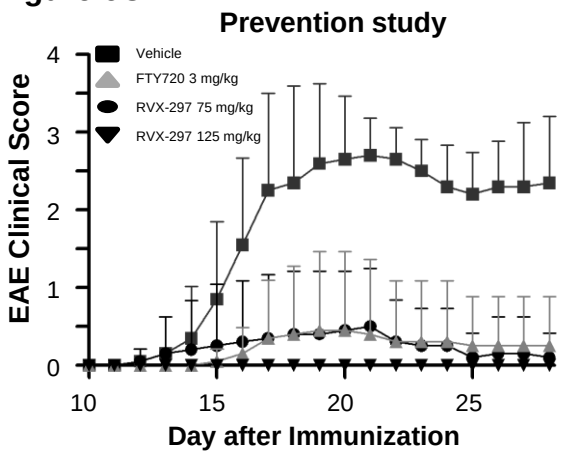

Figure 6D:

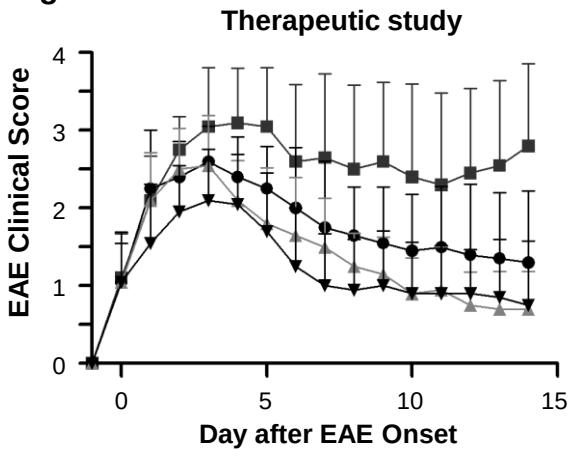

Figure 6E:

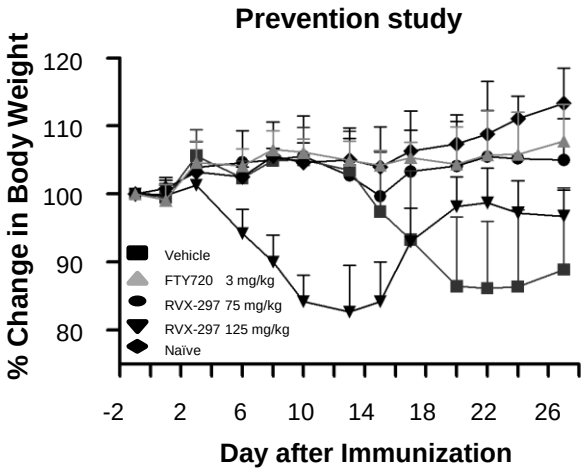

Figure 6F:

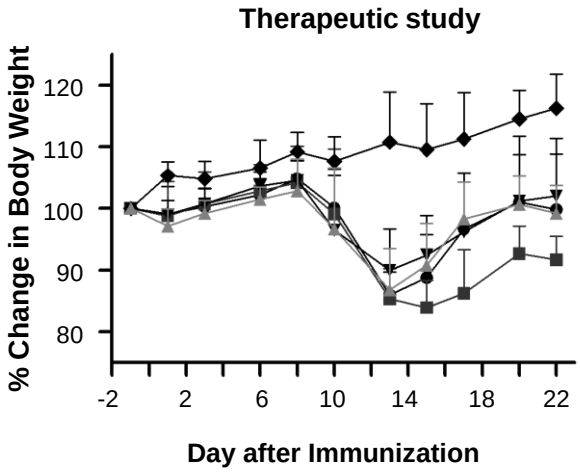

Figure 6G:

Prevention study

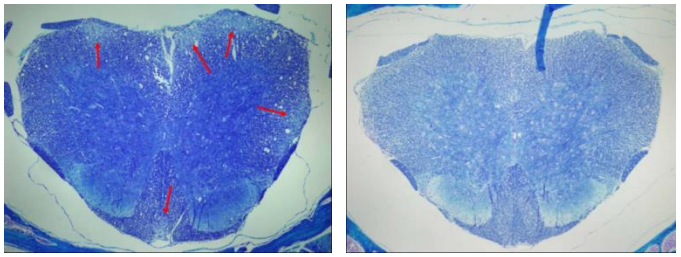

Vehicle | RVX-297, 75 mg/kg

Figure 6H:

Therapeutic study

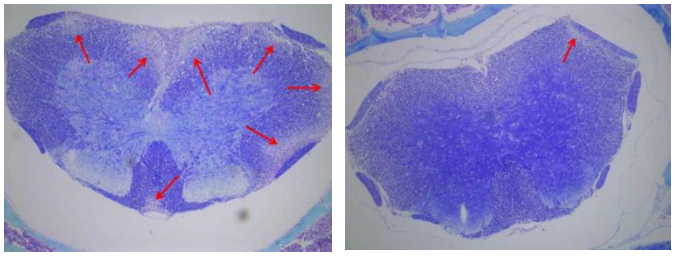

Vehicle | RVX-297, 150 mg/kg

Figure 7:

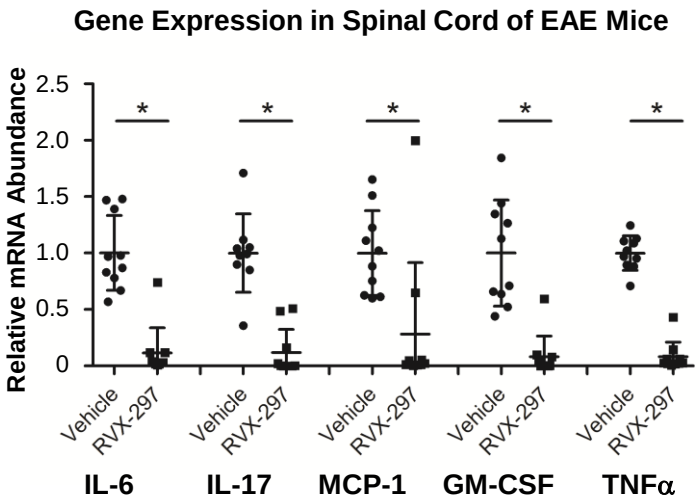

Figure 8: